Accepted Manuscript

Identification of microplastics using Raman spectroscopy: latest developments and future prospects

Catarina F. Araujo, Mariela M. Nolasco, Antonio M.P. Ribeiro, Paulo J.A. Ribeiro-Claro

PII:	S0043-1354(18)30442-1
DOI:	10.1016/j.watres.2018.05.060
Reference:	WR 13825
To appear in:	*Water Research*
Received Date:	08 March 2018
Accepted Date:	31 May 2018

Please cite this article as: Catarina F. Araujo, Mariela M. Nolasco, Antonio M.P. Ribeiro, Paulo J.A. Ribeiro-Claro, Identification of microplastics using Raman spectroscopy: latest developments and future prospects, *Water Research* (2018), doi: 10.1016/j.watres.2018.05.060

Identification of microplastics using Raman spectroscopy: latest developments and future prospects

Catarina F. Araujo[1*], Mariela M. Nolasco[1], Antonio M.P. Ribeiro[1], Paulo J.A Ribeiro-Claro[1*]

[1]*CICECO – Aveiro Institute of Materials, Departamento de Química, Universidade de Aveiro, 3810-193 Aveiro, Portugal.* *catarina.araujo@ua.pt, *prc@ua.pt

Abstract

Widespread microplastic pollution is raising growing concerns as to its detrimental effects upon living organisms. A realistic risk assessment must stand on representative data on the abundance, size distribution and chemical composition of microplastics. Raman microscopy is an indispensable tool for the analysis of very small microplastics (< 20 μm). Still, its use is far from widespread, in part due to drawbacks such as long measurement time and proneness to spectral distortion induced by fluorescence. This review discusses each drawback followed by a showcase of interesting and easily available solutions that contribute to faster and better identification of microplastics using Raman spectroscopy. Among discussed topics are: enhanced signal quality with better detectors and spectrum processing; automated particle selection for faster Raman mapping; comprehensive reference libraries for successful spectral matching. A last section introduces non-conventional Raman techniques (non-linear Raman, hyperspectral imaging, standoff Raman) which permit more advanced applications such as real-time Raman detection and imaging of microplastics.

Keywords

Small microplastics; Automation; Fluorescent tagging; Library matching; Real-time analysis; Stimulated Raman Scattering;

1. Introduction

The advent of synthetic plastics ushered in a golden era of unprecedented technological advancement and improved levels of material comfort, perfectly summed in the classic DuPont slogan "Better Living Through Chemistry". Yet, this euphoric period of unbridled techno-optimism inevitably abated in tandem with growing concerns regarding the harmful impacts of plastic waste, among them the plight of widespread microplastic pollution in the biosphere. According to a recent estimate there are currently more than 5 trillion plastic particles floating at sea, totalling circa 270 000 tonnes (Eriksen et al., 2014). As plastic degradation proceeds and each particle fragments into ever smaller pieces, the total number of particles gallops upwards in an exponential fashion – and so do the risks they pose to animal and human life (Avio et al., 2017; Karami et al., 2016; Ogonowski et al., 2018; Revel et al., 2018; Wright and Kelly, 2017).

Microplastics (MPs), defined as plastic particles ranging from 1 μm to 5 mm in size, are now ubiquitously present in aquatic and terrestrial environments (Duis and

Coors, 2016; Horton et al., 2017b) – often finding their way into our food and drink (Alexander et al., 2016; Karami et al., 2018; Schymanski et al., 2018). A realistic assessment of the ill effects of MPs must commence with a representative, large scale analysis of their abundance, size distribution and chemical composition (Jahnke et al., 2017). Towards this end, chemistry provides a set of identification tools capable of tackling the MP issue in its many facets (Hanvey et al., 2017; Shim et al., 2017; Silva et al., 2018) such as vibrational spectroscopy, densitometry, differential scanning calorimetry (DSC), gas chromatography-mass spectrometry (GC-MS) based methods and the recently proposed technique hyperspectral imaging (Shan et al., 2018).

This review focuses on a particular characterization technique – Raman spectroscopy – which is rapidly gaining ground in the analysis of small MPs. Raman spectroscopy is a vibrational spectroscopy technique based on the inelastic scattering of light that provides information upon the molecular vibrations of a system in the form of a vibrational spectrum. The Raman spectrum is akin to a fingerprint of chemical structure allowing identification of the components present in the sample.

Some of the advantages of Raman spectroscopy are shared by FT-IR techniques, such as non-destructiveness, low sample amount requirement, possibility for high throughput screening and environmental friendliness. These are relevant advantages over other reported methods (i.e. DSC, Pyr-GC-MS) for MPs analysis and characterization (Elert et al., 2017; Ribeiro-Claro et al., 2017). Indeed, vibrational spectroscopy is a common choice for MP identification and has been recommended by the European Union expert group on marine litter, who advocate that all suspected MPs in the 1-100 μm size range should have their polymer identity confirmed by spectroscopic analysis (Gago et al., 2016).

Compared with FTIR spectroscopy, Raman techniques show better spatial resolution (down to 1 μm while that of FTIR is 10-20 μm), wider spectral coverage, higher sensitivity to non-polar functional groups, lower water interference and narrower spectral bands. On the downside, Raman spectroscopy is prone to fluorescence interference, has an inherently low signal to noise ratio and might cause sample heating due to the use of a laser as light source, leading to background emission occasionally followed by polymer degradation. A more comprehensive explanation of the theoretical principles of Raman spectroscopy, its strengths and weaknesses for MP analysis, as well as instrumentation details can be found elsewhere (Ivleva et al., 2017; Ribeiro-Claro et al., 2017; Silva et al., 2018; Smith and Dent, 2005).

Despite its many advantages, the identification of MPs through the use of Raman spectroscopy is yet to attain the popularity of FT-IR techniques, although the number of publications is steeply increasing. At this juncture (May 2018), a search on ISI Web of Knowledge, ResearchGate and ScienceDirect yields a total of 71 original articles on MP identification using Raman spectroscopy. Out of these, 86% employ Raman microscopy (μ-Raman) – the classical Raman setup was only used in early studies and since then discontinued. The surveyed works are listed and grouped into handy categories, in Table 1. Additionally, 6 book chapters and 21 reviews cover the topic with varying levels of detail, with one book chapter from (Ribeiro-Claro et al., 2017) completely dedicated to it. Yet, the significant boom in μ-Raman detection of MPs that took place since then warrants an updated digest of current limitations and emerging solutions. Before delving into that, it is useful to demonstrate why Raman spectroscopy is essential for the study of very small MPs, a domain where FTIR techniques are wholly inadequate.

94 Table 1 – Comprehensive list of documents dealing with MP analysis through
95 Raman, as of January 2018

Reference guide for works on Raman identification of microplastics	
in seawater, freshwater and wastewater	(Cozar et al., 2014; De Tender et al., 2015; Di and Wang, 2018; Enders et al., 2015; Erni-Cassola et al., 2017; Frere et al., 2017, 2016; Ghosal et al., 2018; Karlsson et al., 2017; Lares et al., 2018; Lenz et al., 2015; Lusher et al., 2014; Sujathan et al., 2017; Xiong et al., 2018; Yonkos et al., 2014; Zettler et al., 2013; Zhang et al., 2017; Zhao et al., 2017, 2015)
in sediment	(Ballent et al., 2016; Clunies-Ross et al., 2016; De Tender et al., 2015; Di and Wang, 2018; Elert et al., 2017; Erni-Cassola et al., 2017; Fischer et al., 2015; Horton et al., 2017a; Imhof et al., 2018, 2016, 2013, 2012; Kaeppler et al., 2016; Karlsson et al., 2017; Lots et al., 2017; Maes et al., 2017; Scheurer and Bigalke, 2018; Shan et al., 2018; Sruthy and Ramasamy, 2017; Van Cauwenberghe et al., 2013; Xiong et al., 2018; Young and Elliott, 2016; Zada et al., 2018; Zhang et al., 2017, 2016)
in aquatic organisms	(Cole et al., 2013; Collard et al., 2017a, 2017b, 2015; Dehaut et al., 2016; Enders et al., 2017; Galloway et al., 2017; Ghosal et al., 2018; Goldstein and Goodwin, 2013; Halstead et al., 2018; Horton et al., 2018; Karami et al., 2017b, 2016; Karlsson et al., 2017; Liboiron et al., 2018; Murray and Cowie, 2011; Naidu et al., 2018; Remy et al., 2015; Van Cauwenberghe et al., 2015; Van Cauwenberghe and Janssen, 2014; Wagner et al., 2017; Watts et al., 2016, 2014; Xiong et al., 2018)
in food, drink and cosmetics	(Gündoğdu, 2018; Karami et al., 2017a, 2017c, 2018; Lei et al., 2017; Muhlschlegel et al., 2017; Schymanski et al., 2018; Van Cauwenberghe and Janssen, 2014; Wiesheu et al., 2016; Zada et al., 2018)

Model/Reference samples	(Cai et al., 2018; Kaeppler et al., 2015; Karami et al., 2016; Ossmann et al., 2017; Zada et al., 2018)
Reviews and book chapters	(Andrady, 2017; Blaesing and Amelung, 2018; Crawford and Quinn, 2017; da Costa et al., 2016; Duis and Coors, 2016; Hanvey et al., 2017; Hidalgo-Ruz et al., 2012; Horton et al., 2017b; Ivleva et al., 2017; Jiang, 2018; Klein et al., 2018; Li et al., 2017; Loeder and Gerdts, 2015; Lusher et al., 2017; Mai et al., 2018; Miller et al., 2017; Qiu et al., 2016; Renner et al., 2018; Ribeiro-Claro et al., 2017; Rocha-Santos and Duarte, 2015; Rodríguez-Seijo and Pereira, 2017; Shim et al., 2017; Silva et al., 2018; Syakti, 2017; Wu et al., 2018; Yu et al., 2018)

2. The importance of going small

It might be argued that, relative to μ-FTIR, the most attractive feature of μ-Raman is higher resolution, which becomes especially relevant for identifying very small MPs (< 20 μm) (Elert et al., 2017; Ivleva et al., 2017; Kaeppler et al., 2016) otherwise undetectable using infrared techniques. As detailed in this section, there is an urgent need for a fast and easily implementable monitoring tool capable of detecting small MPs.

Plastic particles exposed to environmental stressors undergo continuous fragmentation (photo-, thermal and biodegradation), so that the number of particles is expected to increase steeply for smaller sizes (Andrady, 2017; Cozar et al., 2014). Despite this fact, the smaller fraction of MPs has been consistently neglected in quantification studies. Conkle *et al.* (Conkle et al., 2018) reviewed 41 surveys of aquatic

MPs in which plastic debris were collected using neuston nets. Circa 80% of these studies used nets with relatively large mesh size (≥ 300 μm), thus entirely missing the smaller MP fraction and leading to a severe underestimation of the actual MP load in aquatic environments. Likewise, a long-term study (Beer *et al.*, 2018) on MP concentration in the Baltic Sea, spanning three decades, used a bongo net with mesh size 150 μm and did not find a significant increase in MP abundance between 1987 and 2015. The results might have been different for the MP fraction below 150 μm. As highlighted in a study by Enders *et al.* (Enders et al., 2015), among small MPs (<400 μm) collected in the Atlantic Ocean and identified using μ-Raman, 64% are under 40 μm in size, and their distribution in the range 10-100 μm follows a power law with a scaling exponent of 1.96, as depicted in Figure 1.

[INSERT FIGURE 1 HERE]

Figure 1 - Particle size distribution of MPs collected in the Atlantic ocean (np=543). Dark grey bars represent particles by length. Light grey bars show the size as geometric mean of length and width. Insets show the smallest (left) and largest (right) MP particles found and confirmed via μ-Raman. Reprinted from Marine Pollution Bulletin, 100, K. Enders, R. Lenz, C.A. Stedmon, T.G. Nielsen, Abundance, size and polymer composition of marine microplastics ≥10μm in the Atlantic Ocean and their modelled vertical distribution, 70-81, Copyright 2015, with permission from Elsevier.

These findings are supported by the conclusions of Erni-Cassola *et al.*, (Erni-Cassola et al., 2017, p.) who also used μ-Raman to identify MPs (<400 μm) from the surface water of Plymouth Bay (UK), determining that the fraction of MPs smaller than 40 μm accounts for roughly 50% of the total population. Therefore, properly measuring the abundance of MPs smaller than 40 μm is of paramount importance when estimating the total MP load in the environment. Moreover, MP identification is increasingly

becoming a consumer health issue. In a recent statement (Alexander *et al.*, 2016), the European Food Safety Authority (EFSA) acknowledged the lack of legislation for microplastics and nanoplastics as contaminants in food and the need to develop reliable identification methods, especially for smaller MPs, which present a higher chance of translocation across the gut barrier . Indeed, μ-Raman analysis has found MPs in edible fish tissues (Collard et al., 2017a; Karami et al., 2017c, 2018), table salt (Gündoğdu, 2018; Karami et al., 2017a) and bottled water (Schymanski *et al.*, 2018). The latter study, by Schymanski and co-workers, analysed 38 brands of bottled water (plastic, carton and glass containers) and found MP contamination in all of them, with 80% of found particles belonging to the 5-20 μm size range. A comparison of FTIR and Raman techniques for MP identification, performed by Käppler *et al.* (Kaeppler et al., 2016), illustrates the superior performance of μ-Raman for detecting small MPs. While for particles larger than 20 μm both techniques proved equally capable, for smaller particles the detection success rate of μ-FTIR lagged behind. μ-Raman detected MPs as small as 5 μm, yet μ-FTIR missed all particles in the 5-10 μm size range and 40% of MPs in the 11-20 μm size range. Moreover, even though μ-FTIR did succeed in identifying some MPs in the 11-20 μm range, the quality of the spectra suffered due to low signal to noise ratio – a direct consequence of the size of the particle approaching that of the instrument's diffraction limit. This issue is illustrated by comparing the FTIR and Raman spectra of a small (15-20 μm) polypropylene (PP) particle, as shown in Figure 2b, where a clear Raman spectrum (left) contrasts with a weak and noisy FTIR spectrum (right).

[INSERT FIGURE 2 HERE]

Figure 2 – a) Raman image (left) and IR image (right) with false-colouring denoting the spectral intensity in the 2780–2980 cm^{-1} range. B) Raman spectrum (left) and IR transmission spectrum (right) of particle 2 in comparison with a reference of polypropylene. Adapted by permission from Springer Nature Analytical and Bioanalytical Chemistry, Analysis of environmental microplastics by vibrational microspectroscopy: FTIR, Raman or both?, A. Käppler, D. Fischer, S. Oberbeckmann *et al.*, Copyright 2016.

The efficiency of an ingenious post-filtration system implemented in the wastewater treatment plant of Oldenburg (Germany) was evaluated by comparing the amount of MPs present in wastewater samples collected upstream and downstream from the filtration point (Mintenig *et al.*, 2017). A removal efficiency of 100% was reported for MPs > 500 μm and of 93% for those < 500 μm. Given that the filtration system consists of pile fabric with a mesh size of 10-15 μm and that particles smaller than 20 μm could not be detected using FTIR imaging, a significant portion of very small MPs might be passing through unnoticed. Being so, FTIR imaging studies should be complemented by μ-Raman for properly accounting for MPs in the smaller size range. However, μ-Raman is not used in the majority of MP identification studies (14% according to a recent review (Renner *et al.*, 2018)) in great part due to its cumbersomeness (e.g. fluorescence masking) and long measurement time. Certainly, the shortcomings of μ-Raman must be overcome prior to its large scale implementation. Recently, a considerable effort has been made to optimize signal quality (section 3) and automation routines (section 4) that enable faster and more reliable μ-Raman identification of MPs.

3. Enhancing signal quality

187

188 Two commonly cited drawbacks of classical Raman scattering as a method for
189 MP analysis are the inherent weakness of the signal – only about 10^{-8} of the photons
190 bombarding the sample are actually translated to Raman signal (Borman, 1982) – and
191 its proneness to fluorescence interference – either intrinsic to the main constituent of the
192 MP or due to impurities such as colouring agents, biological material and degradation
193 products. A weak signal imposes the necessity of extending the integration time which,
194 in the best case scenario, increases the duration of the measurement, and in the worst
195 case scenario results in laser-induced degradation of the sample. Fluorescence results in
196 a raised baseline which, in the worst cases, completely overshadows the Raman signal.
197 There are many possible routes to minimize these problems. A radical approach is to
198 forego spontaneous Raman scattering in favor of nonlinear Raman techniques, which by
199 their very nature offer high signal to noise ratio while being free from the interference
200 of fluorescence (Borman, 1982). However, nonlinear Raman methods require expensive
201 equipment and expert user knowledge so that their implementation in MP analysis is
202 still incipient (Cole et al., 2013; Galloway et al., 2017; Watts et al., 2016, 2014; Zada et
203 al., 2018). The present section focuses instead on offering examples of recently
204 suggested good practices designed to minimize the weak signal and fluorescence
205 problems of spontaneous Raman spectroscopy.

206 In the specific context of MP analysis, an obvious way of reducing fluorescence
207 caused by organic debris – and, in some cases, by organic dyes - is the use of an
208 appropriate cleaning protocol to remove the contaminants. Among the pre-treatments
209 proposed for cleaning MPs are those employing acids, bases, oxidative and enzymatic
210 agents, as extensively discussed in a series of recent reviews (Blaesing and Amelung,
211 2018; Lusher et al., 2017; Miller et al., 2017, 2017; Renner et al., 2018; Silva et al.,

2018). Worthy of mention is the benchmark study of Dehaut *et al.* (Dehaut et al., 2016) which assessed the efficiency and degradation effect of six digestion methods. The authors concluded that digestion with nitric acid, at the time the official method recommended by the International Council for the Exploration of the Sea (ICES), leads to significant polymer degradation and consequent MP underestimation. Instead, the authors recommended digestion in a 10% KOH solution. Similar conclusions were reached by Enders *et al.* (Enders et al., 2017), who confirm the destructive effects of nitric acid digestion and, in partnership with ICES, issued a new official recommendation for MP cleaning using a mixture of 30% KOH:NaClO Alternatively, an enzymatic digestion method employing proteinase K efficiently cleaned samples of salmon viscera and fecal matter, spiked with MPs, without significant polymer degradation (Karlsson *et al.*, 2017).

Alas, even after thorough cleaning, some samples will exhibit a problematic degree of fluorescence, mainly due to the presence of hard to remove colouring agents. A commonly cited solution is photo-bleaching the sample, that is, placing it under the laser for the time necessary for degrading the fluorescing agent. However, besides being time consuming, this strategy cannot be applied to samples prone to photo-degradation or pyrolysis – and even when applied it does not always work. A speedy solution for enabling correct identification of fluorescing samples is proposed by Ghosal *et al.* (Ghosal et al., 2018) who use an automated algorithm to remove the fluorescence background and reveal the underlying polymer spectrum. A striking example of the algorithm's effectiveness is shown in Figure 3 depicting a plastic particle partially covered in biofilm and Raman spectra collected at covered (red) and bare (black) locations. Prior to background subtraction the spectrum of the covered surface is saturated with the fluorescence signal which completely overshadows the characteristic

polymer peaks. After processing, the polymer peaks are clearly visible, allowing polymer identification by a library matching software. The source code for the algorithm, which includes a graphical user interface, is freely available at https://github.com/michaelstchen/modPolyFit.

[INSERT FIGURE 3 HERE]

Figure 3 – Raman spectra of a polyethylene (PE) particle partially covered in biofilm. The characteristic PE peaks readily apparent in the raw spectrum collected from the bare plastic surface (black line, upper panel) seem to be absent from the raw spectrum of the biofilm-covered plastic surface (red line, upper panel). After automated fluorescence correction, the spectral fingerprint of PE clearly emerges in the processed spectrum of the biofilm-covered plastic surface (red line, lower panel). Adapted from Environmental Pollution, 233, S. Ghosal, M. Chen, J. Wagner, Z. Wang, S. Wall, Molecular identification of polymers and anthropogenic particles extracted from oceanic water and fish stomach – A Raman micro-spectroscopy study, 1113-1124, Copyright 2018, with permission from Elsevier.

An additional source of fluorescence may be the substrate underneath the MPs (i.e. the filter), as noted by Oßmann *et al.* (Ossmann et al., 2017) who compared the performance of six commercial filters commonly used for µ-Raman analysis and custom made polycarbonate substrates coated with three different metals. The filter offering the best performance is made of polycarbonate coated with aluminum, which not only minimizes fluorescence and burning of the sample but also optimizes optical contrast between filter and MPs, thereby easing automated particle search.

As mentioned before, a drawback of Raman spectroscopy is the notoriously weak intensity of Raman scattering, which requires relatively long acquisition times to achieve a decent signal to noise ratio. One avenue for signal enhancement arises from the development of improved detector systems – as illustrated by the comparison

between conventional and electron-multiplying charged coupled device detectors (CCD vs. EM-CCD). Relative to conventional CCD detectors, EM-CCD detectors are equipped with a multiplication register that acts prior to the readout – amplifying the gain up to 1000 times (Andor Technology, 2007; Griffiths and Miseo, 2014). As a result, EM-CCD detectors are expected to require less acquisition time to achieve the same signal to noise ratio as conventional CCD detectors, rendering the former especially relevant for fast Raman mapping and imaging applications (Griffiths and Miseo, 2014). The power of EM-CCD detectors applied to Raman characterization of MPs is clearly illustrated by work of Dieing and Hollricher, from which Fig. 4 has been retrieved (Dieing and Hollricher, 2008). Figure 4a) depicts the Raman image of contaminated poly(methyl methacrylate) (PMMA) on a glass slide obtained using a classical CCD detector and with an integration time of 36ms/spectrum. The signal to noise ratio is low, so that one can barely distinguish the vertical stripe in the center (glass) from the side regions (PMMA+impurities). Using a EM-CCD detector, the same signal to noise ratio is achieved in a tenth of the integration time (Figure 4b). By setting the integration time at the same as that used for the CCD detector, a superior image is obtained (Figure 4c), where not only the glass is clearly distinguished from PMMA, but the streaks of impurities are also easily discernible.

[INSERT FIGURE 4 HERE]

Figure 4 - Raman Images of a glass slide, partially covered with a layer of PMMA and contaminant (scheme d), obtained with: (a) back-illuminated CCD; (b and c) EMCCD. Scale bar:10 μm. Reprinted from Vibrational Spectroscopy, 48 (1), T. Dieing, O. Hollricher, High-resolution, high-speed confocal Raman imaging, 22-27, Copyright 2008, with permission from Elsevier.

4. Automated routines for Raman mapping

Until recently, the great majority of studies reporting MP load in environmental samples relied solely upon visual inspection (usually under a microscope) to determine the total number of plastic particles in the analyzed sample. The perils of such approach have been highlighted in the impactful work of Lenz *et al.* (Lenz et al., 2015) who warn that visual inspection alone leads both to false positives (e.g. paint particles) and false negatives (e.g. darkly coloured MPs mistaken for naturally occurring particles). Visual detection relies upon morphological criteria to decide whether a given particle is made of plastic, an approach that works reasonably well for bigger MPs (>100 μm) but progressively fails as MP size diminishes and morphological features become less apparent. Thus, among those MPs <50 μm which were selected under the microscope, only 63% could be confirmed as plastics after Raman analysis (Lenz et al., 2015). As the authors point out, running a FTIR or Raman analysis following visual sorting eradicates the problem of false positives but perpetuates the issue of false negatives. This concern is well expressed in the study of Song *et al.* (Song et al., 2015) which compares the effectiveness of visual pre-sorting under a microscope followed by FTIR analysis with that of analyzing the spectra of all particles present in the sample. While full FTIR analysis always leads to a larger estimate of MP abundance, the contrast is most staggering for particles smaller than 50 μm for which the visual sorting procedure failed to account for roughly half of the MPs detected using FTIR. One may argue that if Raman had been used instead, the difference would be even more striking. It is then

clear that visual pre-sorting, besides taking up far too much operator time, likely leads to less than representative results. An obvious solution to increase representativeness is to analyze every single particle in a given sample, however such approach requires even more operator time than visual pre-sorting. A more viable solution is automated analysis and there are various ways of doing so. One possibility is full point mapping, where a whole filter section is analyzed by collecting spectra at various points along a grid with the aid of a motorized stage which moves the sample under the laser in small increments. While thorough, this approach is rather slow, as illustrated in the work of Käppler *et al.* (Kaeppler et al., 2016), whose point-by-point µ-Raman mapping without pre-selection took a whopping 38 h to scan 1 mm^2 of the sample filter using a point distance of 10 µm and total integration time of 10 sec per point. By reducing the integration time to 0.5 sec per point and using a topographical imaging tool to enhance focus, the total measurement time was reduced to 90 min but the increase in speed came at the expense of detection success rate, which was equivalent to that of the FTIR imaging technique.

The major drawback in point by point mapping for MP analysis is that it does not detect whether there is an actual particle under the laser – the whole grid is scanned, so a good proportion of laser time will be wasted measuring the spectrum of the filter itself. Time can be saved by guiding the laser directly to a small area where a particle is located. Elert *et al.* (Elert et al., 2017) used this approach in their comparison of four techniques (FTIR imaging, Raman mapping, mass spectrometry and chemical extraction) for the analysis of soil spiked with reference MPs. Particles ranging from 150 to 200 µm were visually selected under the microscope and the scanning area adjusted to fit each analyzed particle – an undesirable practice for environmental studies but appropriate for comparison purposes. A pre-scan was run with a short integration

time of 20 ms per point in order to create a spectral image of each particle. Then, higher resolution spectra were collected only at specific points of interest (i.e. a clear spot vs a fluorescing spot). This procedure was more time-efficient than full mapping, taking circa 15 hours per mm^2. Besides, by focusing the analysis on a smaller area, a shorter size step could be used (1 μm) so that different chemical compositions at the particle surface could be distinguished. While this approach is valuable for in-depth studies, routine monitoring protocols must be swifter.

An interesting strategy is the use of image analysis software which, by enhancing contrast between particles and filter, creates a map of all particles in a given area and Raman spectra are collected only at those points. Schymanski *et al.* (Schymanski et al., 2018) used the Single Particle Explorer (rapID) software to automatically detect particles larger than 5 μm up to a maximum of 5000 particles per scanned area. Chemical identification was achieved by library matching and all MPs with a ranking score between 550 and 700 were then individually analyzed using longer integration times to improve signal to noise ratio. Despite the time consuming verification step, the analysis was performed at a rate of 56 min/mm^2, a significant improvement relative to point mapping approaches. Frère *et al.* (Frere et al., 2016) achieved an even shorter measurement time of $20s/mm^2$ by performing an automated particle search using the ParticleFinder (Horiba) software and collecting the spectrum of each detected particle. The higher speed efficiency of this measurement relative to that of Schymanski's study has to do with the size of the MPs sampled (> 300 μm) and the absence of a thorough verification step, a comparison which nicely illustrates the trade-off between meticulousness and celerity. An optimized software for the automated detection of particles and fibres in the 1 μm – 500 μm range is currently being developed by Käppler and colleagues, within the framework of the project

MICROPOLL - EU BONUS program (Oberbeckmann, 2017), which might allow a more thorough analysis in a shorter time scale.

A truly innovative approach is the method for MP detection using a fluorescent dye, initially suggested by Andrady (Andrady, 2011) and demonstrated in recent works (Erni-Cassola *et al.*, 2017; Maes *et al.*, 2017; Shim *et al.*, 2016), which currently yields the best compromise between speed and accuracy . Nile Red, a solvatochromic fluorescent dye, was found to selectively stain synthetic polymers – but not tire rubber - enabling their fast detection under a UV light, as depicted in Figure 5.

[INSERT FIGURE 5 HERE]

Figure 5 - Microscope images of a) polyethylene, b) nylon 6 and c) rubber stained with Nile red. Left panel: brightfield images, center and right panels: fluorescent image at excitation/emission 460/525 nm (green) and 565/630 nm (red), respectively. Scale bar is 125 µm. Adapted with permission from Environmental Science & Technology, 51, G. Erni-Cassola, M.I. Gibson, R.C. Thompson, et al., Lost, but Found with Nile Red: A Novel Method for Detecting and Quantifying Small Microplastics (1 mm to 20 µm) in Environmental Samples, 13641−13648, Copyright 2017 American Chemical Society.

This procedure might seem counterproductive, as the fluorescence induced by the dye may mask the Raman signal. However, one author (Maes *et al.*, 2017) claims that "The very small amounts of Nile Red adsorbed on the particles did not interfere with IR or Raman spectroscopy" while another (Erni-Cassola *et al.*, 2017) reports an undesirable level of interference. The authors minimize the deleterious effects of fluorescence by photo-bleaching the sample for 5 min prior to Raman analysis. The great advantage of this method lies in the particle selection stage, where an automated particle search is applied using imaging software and detecting only fluorescing

particles, so that only a fraction of the particles initially present (under 10%) are selected for further analysis. Not all of the stained particles are necessarily plastics – non-plastic fragments contaminated with hydrophobic biological material are stained as well. However their detection can be minimized by combining an effective cleaning step (prior to Nile Red staining) and the use of a UV wavelength that induces green instead of red fluorescence – plastic particles fluoresce better in green while organic material does not (Erni-Cassola *et al.*, 2017).

Following this strategy, Erni-Cassola and co-workers located MPs as small as 20 μm and determined their chemical composition using μ-Raman totaling a measurement time of almost 2 minutes per mm^2. If the photo-bleaching step had been omitted, the total analysis time would be roughly 40 seconds per mm^2. A more time-efficient procedure would be to: 1) run a first test without photo-bleaching MPs; 2) run the raw spectra through an automated baseline correction script (Ghosal *et al.*, 2018); 3) attempt automatic identification through library matching and 4) photo-bleach and re-analyze only those particles which could not be successfully identified in the first run.

The aforementioned studies of MP identification using μ-Raman have all relied on a mapping – or "point and shoot" – strategy which collects spectra one point at a time. However, it is already possible to image a whole area in a single scan using widefield techniques, as discussed in section 6. Such strategy is often implemented for FTIR analysis of MPs using a focal plane array (FPA) detector. Imaging a whole area in a single measurement promises gains in expediency and representativeness by dispensing with the step of particle selection and the use of a motorized stage. Yet, at present, FTIR imaging with FPA is not necessarily more time-efficient than Raman mapping. The measurement time/mm^2 of a few selected works employing either Raman mapping or FPA to detect MPs are presented in Table 2. Both categories showcase

412 examples in which 1 mm^2 of sample area was analyzed within a few minutes, and even
413 seconds. On top of being comparable to FTIR imaging in terms of analysis time, Raman
414 mapping offers the possibility of identifying MPs in the 1-20 µm range. This
415 competitive "edge" of Raman mapping is likely to fade in coming years, as
416 advancements in instrumentation deliver affordable and time-efficient devices for
417 proper Raman imaging.

418

419

420 Table 2 – Comparison of studies employing automated routines for MP identification using µ-Raman and
421 µ-FTIR. The total analysis time per mm^2 was calculated based on the total measurement time reported by
422 the authors divided by the measured area.

Ref.	Technique	Protocol	Min. particle size detected	Int. time /point	Total analysis time per mm^2
(Kaeppler *et al.*, 2016)	µ-Raman *alpha 300R Raman microscope (WITec)*	*- No pre-selection -Automated scanning of the whole filter area in 10 µm steps -ID by automated library matching*	5 µm	10 s	38 h/mm^2
((Elert et al., 2017)	µ-Raman *alpha 300R Raman microscope (WITec)*	*-Visual pre-selection of potential MPs -Automated scanning of small filter sub-sections (max: 0.2 x 0.19 mm) in 1 µm steps -ID by comparison with ref spectra*	150 µm	0.02 s	15 h/mm^2 + pre-selection time
(Schymans	µ-Raman	*-Automated particle search by*	5 µm	5 s	56 min/mm^2

ki *et al.*, 2018)	*Single Particle Explorer (rapID)*	*the Single Particle Explorer -Raman spectra collected at each particle location -ID by automated library matching followed by individual verification of low confidence matches*			
(Frere *et al.*, 2016)	µ-Raman *LabRAM HR800 (Horiba Scientific)*	*-Automatic particle search by the ParticleFinder software -Raman spectra collected at each particle location -ID by automated library matching*	300 µm	20 s	20 s/mm^2
(Erni-Cassola *et al.*, 2017)	µ-Raman *inVia Raman microscope (Renishaw)*	*-Staining with fluorescent dye followed by automatic particle search by the ImageJ software -Raman spectra collected at each particle location -ID method not specified*	20 µm	200 s	~2 min/mm^2*
(Elert *et al.*, 2017)	µ-FTIR *Vertex 70 spectrometer (Bruker)*	*Use of a focal plane array for direct imaging of a whole filter section*	100 µm	-	111 min/mm^2
(Kaeppler *et al.*, 2016)	µ-FTIR *Tensor 27 spectrometer (Bruker)*	*Use of a focal plane array for direct imaging of a whole filter section*	15 µm	-	20 min/mm^2
(Loeder *et al.*, 2015)	µ-FTIR *PerkinElmer Spotlight micro-FT-IR*	*Use of a focal plane array for direct imaging of a whole filter section*	20 µm	-	6 min/mm^2

(Tagg *et al.*, 2015)	μ-FTIR *Tensor 27 spectrometer (Bruker)*	*Use of a focal plane array for direct imaging of a whole filter section*	150 μm	-	19 s/mm^2 (1 scan) 33 s/mm^2 (2 scans)

*The authors only disclosed the time necessary for particle detection (2.45 s/mm2) so the total analysis time was estimated based on the time necessary to measure all the analyzed particles (199x200s) plus the pre-measurement bleaching step (199x5min) divided by the total scanned area (23 sections of 23x1.8 mm each)

5. Spectral Libraries

Automated μ-Raman routines employ library matching software to compare the spectrum of the sample with that of custom made and/or commercial libraries. The likelihood of successful matching greatly depends upon the comprehensiveness of the spectral library. However, custom made libraries usually rely on spectra acquired from pristine polymer pellets and may differ significantly from those of MPs collected from environmental compartments. Environmental MPs mostly result from the fragmentation of commercial polymers, available in different morphologies (foam, sheet, fibre) and include in their composition a variety of additives, fillers and colouring agents. These components, in some instances, overlay or even mask the underlying polymer spectrum. The use of more comprehensive commercial libraries is a step in the right direction to enhancing matching scores, especially if the matching algorithm uses multicomponent correlations (Lenz *et al.*, 2015). Among 31 studies using automated matching software for MP identification, 6 rely solely on custom made reference libraries, 13 used solely commercial libraries (although most of them use a collection of libraries from different

444 vendors) and 12 use a combination of commercial and custom made libraries. The need
445 for different commercial libraries, often complemented with own reference spectra is a
446 good indicator that no single commercial library is currently broad enough to assure
447 extensive success rates. Perhaps part of this problem is due to the fact that both
448 commercial and custom made libraries only include spectra from plastics that were not
449 exposed to environmental degradation.

450 MPs in the environment are continuously exposed to a variety of environmental
451 stressors (UV light, heat, biodegradation) that result in plastic weathering (Andrady,
452 2017; Lenz *et al.*, 2015). For example, polyvinylchloride (PVC) is prone to photo-
453 degradation in aquatic media, as the leakage of additives, such as photo-stabilizers,
454 accelerates under high humidity conditions. UV degradation significantly alters the
455 spectral fingerprint of PVC showing a simultaneous intensity decrease of the
456 neighboring peaks at 693 cm^{-1} and 637 cm^{-1}, which stem from the characteristic C-Cl
457 bonds of the polymer (Lenz et al., 2015). For the spectrum corresponding to the highest
458 UV exposure, a complete absence of these double peaks and the appearance of two
459 strong peaks at 1139 cm^{-1} and 1540 cm^{-1}, assigned to carbon double bonds (C=C), are
460 observed. A successful match through library search was impossible since the only
461 reference for PVC was that of a pristine (non-degraded) sample. In the light of this
462 drawback, it is of utmost importance that spectra of degraded polymers at different
463 degradation stages be included in the reference library, thus increasing the chance of the
464 matching software correctly identifying the polymeric composition. It should however
465 be noted that photo-oxidation is not as problematic for MP identification using Raman
466 as it is when using FTIR techniques. Photo-oxidation of the most common polymers
467 (i.e. PE, PP) results in the formation of oxygenated moieties, chiefly C=O and –OH,
468 which display strong intensities in the infrared spectrum (Andrady, 2017; Cai et al.,

2018; Costa et al., 2018; Rodrigues et al., 2018), contrasting with their typically weak Raman signals. For example Cai et al. (2018) found obvious differences among the infrared spectra of pristine and degraded PE, PP and PS while the corresponding Raman spectra only registered slight differences in band intensities. This feature of Raman may be considered as an advantage – when the purpose is to simply identify plastic identity – or a disadvantage – for those studies focused on assessing the extent of polymer degradation.

Moreover, as Lenz and colleagues have done, it is of value to include the spectra of non-plastic materials which are often confused with MPs, such as cellulose, keratin, inorganic particles and, most important of all, synthetic fibres (i.e. viscose), whose presence is ubiquitous among MP samples. The obvious hurdle with this approach is that it is time consuming for each individual laboratory to build a comprehensive spectral library. An open source, curated spectral database would be of great utility: the effort and material resources spent by each individual researcher would be minimized by avoiding repetition (i.e. each group having to build their own library) while achieving a degree of complexity and completeness currently unavailable in a single commercial library. The inclusion of spectra from real environmental samples, whose identity, when in doubt, could be confirmed through other identification techniques, would greatly increase matching scores. Besides, having access to a free library would encourage more MP identification studies for research groups with narrow funding, thereby expanding our current perception of global MP pollution. Such an enterprise might seem far-fetched, however an open source database for mass spectra – Curatr - has been developed at the European Molecular Biology Laboratory, Germany, (Palmer *et al.*, 2017) and is available at http://curatr.mcf.embl.de/about/curatr/. The spectra uploaded by authorized curators are converted into a format compatible with library

matching software so that any user can easily download and use them in their own studies.

Finally, an interesting way of optimizing automated identification of MPs with complex composition might be using the Raman barcode strategy outlined by Lawson and Rodriguez ((Lawson and Rodriguez, 2016) for the fast identification of counterfeit drugs. Briefly, both reference (APIs) and sample (counterfeit drug) spectra are converted into a barcode where each line represents a spectral peak, as illustrated in Figure 6. The barcode of the sample is then identified through binary comparison with the reference barcodes, thus speeding up matching and dispensing with spectral intensity normalization. The barcode strategy has not yet been applied for the identification of microplastics although it could easily be adapted for that purpose: the reference barcodes would be those of polymers, colouring agents and common plastic additives. The advantage of using the barcode for Raman spectral matching is that ignoring spectral intensity would improve the identification rates for those MPs whose spectra are overshadowed by the peaks of the colouring agent and/or additives.

[INSERT FIGURE 6 HERE]

Figure 6 – Illustration of the Raman barcode generation: peaks marked with a circle are included as vertical stripes in the barcode spectrum. Reprinted with permission from Analytical Chemistry, 88, L.S. Lawson, J.D. Rodriguez, Raman Barcode for Counterfeit Drug Product Detection, 4706−4713. Copyright 2016 American Chemical Society.

519

520 6. Future prospects – emerging non-conventional Raman
521 techniques

522

523 This section discusses non-conventional Raman techniques. These are not, at
524 present, commonly used for the identification of environmental MPs yet might grow in
525 importance for MP research as the necessary instrumentation becomes more easily
526 accessible. A theoretical description of unconventional Raman techniques falls outside
527 the scope of this review, having been comprehensively discussed elsewhere (Stewart *et*
528 *al.*, 2012; Opilik *et al.*, 2013). Furthermore, the aim here is not to delineate novel
529 detection protocols but merely bringing the reader's attention to a wider set of possible
530 Raman tools using concrete examples from the available literature.

531 As mentioned before, the majority of works employing μ-Raman for MP
532 detection follows a mapping, point by point strategy. The spectra collected at each
533 spatial location may then be put together to create a Raman image. However, this cannot
534 be considered a true imaging technique. Proper Raman imaging may rely on either
535 spontaneous or nonlinear processes. In spontaneous Raman imaging – wide-field
536 Raman - a whole sample section is illuminated by defocusing the laser and collecting an
537 image in a single measurement, a strategy not yet applied for environmental MP
538 analysis. In contrast, proper FTIR imaging using FPAs for MP detection has been
539 demonstrated before. An interesting example of wide-field Raman imaging is the proof
540 of concept demonstration of Schmälzlin *et al.* (Schmaelzlin et al., 2014), where a fiber-
541 coupled high-performance astronomy spectrograph (MUSE) was used to image
542 polystyrene (PS) (50 μm) and PMMA (100 μm) microshperes scattered on a metal plate.

543 The exposure time was 2 minutes and, after background subtraction and automated
544 fluorescence correction, the area of non-overlapping characteristic peaks was integrated
545 over the sample area to produce the false color images shown in Figure 7. Although the
546 image presents poor spatial resolution the location and size of the PS and PMMA
547 microspheres are clearly defined. The authors themselves warn that this preliminary test
548 is intended to illustrate the lower limit of the technique's capabilities, since the MUSE
549 spectrograph (designed for astrophysical exploration of distant galaxies) had not been
550 optimized for this specific purpose.

551

552 [INSERT FIGURE 7 HERE]

553

554 Figure 7 –Left panel: optical image of plastic microbeads. Center panel: Raman image of PMMA (600
555 cm−1); Right panel: Raman image of PS (1035 cm−1). Scale bar is 50 μm. Reprinted from Sensors, 14, E.
556 Schmälzlin, B. Moralejo, M. Rutowska, *et al.*, Raman Imaging with a Fiber-Coupled Multichannel
557 Spectrograph, 21968-21980, Copyright 2014, under the terms of the Creative Commons Attribution
558 license 3.0.

559

560 The next frontier in MP characterization is real-time analysis of flowing
561 particles. Conventional Raman techniques, based on spontaneous Raman scattering, are
562 unfit for this purpose. The inherently weak scattering intensity results in the necessity of
563 long dwelling times – milliseconds to seconds - to achieve a good signal. However, the
564 improved signal intensity achieved by nonlinear Raman techniques such as coherent
565 anti-Stokes Raman scattering (CARS) and stimulated Raman scattering (SRS) opens up
566 new possibilities for real-time MP analysis. In CARS and SRS, a strong signal is
567 elicited only from the molecular vibrational modes of interest. Thus, the signal is free
568 from fluorescence, even if strongly fluorescing contaminants are present - as long as

569 these are inactive at the frequency of interest, the sample signal will not be influenced.
570 Therefore, a sufficient signal can be acquired quickly and sample preparation becomes
571 less important – an ideal scenario for real time detection of MPs in environmental
572 compartments.

573 The use of CARS for locating MPs within biological organisms has been
574 demonstrated before for zooplankton (Cole *et al.*, 2013) and crabs (Watts *et al.*, 2016,
575 2014), as briefly discussed elsewhere (Ribeiro-Claro *et al.*, 2017), and more recently,
576 fairy shrimp and zebrafish embryos (Galloway *et al.*, 2017). The latter study, by
577 Galloway and colleagues, detected nanoparticles of acrylic co-polymers as small as 80
578 nm, thereby pushing the limit of plastic particle detection from the micro- to the
579 nanoscale.

580 The potential of SRS for fast analysis of MPs did not go unnoticed by the
581 microplastics research community, as demonstrated in a recent proof of principle study
582 by Zada and co-workers (2018). SRS microscopy was used, in a time-efficient manner,
583 to detect and distinguish MPs of five commonly encountered polymers. The analysis
584 was calibrated at six different wavenumbers (Figure 8a), selected by statistical methods
585 to tell apart the MPs from the background while maximizing polymer type
586 discrimination. Figure 8b displays the SRS identification images of model MPs (upper
587 panel) and its respective color maps identifying polymeric composition (lower panel).
588 The technique was successfully applied in the detection of MPs present in glitter nail
589 polish and sediments from the Rhine estuary. Zada et al. report a total SRS analysis time
590 of 2.7 minutes per mm^2, an impressive speed especially when taking into account that
591 there was no particle pre-selection: the whole filter area was scanned for Raman signals.
592 A comparable full mapping analysis using conventional Raman took 38 hours per mm^2,
593 as reported by the same authors. With conventional Raman, short measurement times

ranging from a few seconds to a few minutes per mm^2 are achievable, but only by drastically reducing the number of data collection points through automated particle pre-selection (see Table 2). The advantage of the latter strategy is greater flexibility, since it can detect a broad range of polymer types, while the SRS scheme suggested by Zada and co-workers only identifies the polymer classes included in the calibration step.

[INSERT FIGURE 8 HERE]

Figure 8 – a) Spontaneous Raman spectra of Nylon, PET, PS, PE and PP with circles indicating the wavenumbers used in the SRS analysis. b) Upper panel: SRS identification images of the aforementioned polymers, with unequivocal identification points shown as white. Lower panel: Color coded version of the identification image above. Adapted from (Zada et al., 2018) under a Creative Commons license (https://creativecommons.org/licenses/by/4.0/legalcode)

Zhang *et al.* (C. Zhang et al., 2017) demonstrated the capabilities of SRS coupled with flow cytometry in the fast identification of plastic microspheres. Beads of PMMA and PS, 10 μm in size, were suspended in water and run through a flow cytometry device coupled to a multichannel SRS system (FC-SRS). The FC-SRS prototype includes a custom-built signal amplifier, allowing the collection of a Raman spectrum in merely 5 μs. With the flow speed set to 400 mm/s, ~11 000 microspheres per second were successfully identified, an astonishing detection rate compared with the timescales previously discussed in this review. Figure 9 (left) shows a time-stack SRS image corresponding to 1.8 ms, a short time window during which 8 PMMA and 5 PS beads were identified through their characteristic peaks in the CH stretching region, shown in Figure 9 (right), aided by multivariate curve resolution.

[INSERT FIGURE 9 HERE]

Figure 9 – Left panel: Time stacked window recorded in 1.8 ms, 8 PMMA beads (peak centered at 2955 cm−1) and 5 PS beads (peak centered at 3060 cm−1) were detected. Right panel: SRS (dashed) and spontaneous Raman Spectra (bold) of PMMA and PS. Reprinted from Optica, 4, C. Zhang, K. Huang, B. Rajwa *et al.*, Stimulated Raman scattering flow cytometry for label-free single-particle analysis, 103-109, Copyright 2017, under OSA Open Access License

Combining real time Raman analysis and Raman imaging, Liao et al. (2017) recently proposed a handheld SRS microscope with optical fibre laser delivery that permits *in situ* and *in vivo* chemical identification. The device, depicted in Figure 10, permits imaging at a rate of 8 frames per second, thereby reducing distortion generated by hand movement. The Raman image shown in Figure 10, displaying the spatial locations of PS and PMMA microbeads (5 μm), as well cellulose fibers (from the filter paper underneath) was generated in a mere 3 seconds. Fast, steady and accurate, the handheld SRS device might be an interesting option for real-time monitoring of MPs in food, cosmetics and other consumer products. The handheld device could be suspended above the production line treadmill, attached to an automated arm which scans the surface of the product and rapidly detects the presence of MPs.

[INSERT FIGURE 10 HERE]

Figure 10 –Handheld SRS microscope. Inset: SRS image at 2890 cm-1 of PS/PMMA microspheres on paper (bottom) and output spectra (top). Reprinted with permission from ACS Photonics, C. Liao, P. Wang, C.Y. Huang et al., In Vivo and in Situ Spectroscopic Imaging by a Handheld Stimulated Raman Scattering Microscope, ***Article ASAP,*** *DOI: 10.1021/acsphotonics.7b01214. Copyright 2017 American Chemical Society*

While, in the examples discussed throughout this review, the sample is placed within close reach to the Raman detector, it is possible to collect Raman spectra from afar, at distances up to hundreds of meters. This approach, deemed Standoff Raman spectroscopy, has been developed for detecting samples which are hard to reach and/or dangerous to handle, such as explosives (Gares *et al.*, 2016; Stewart *et al.*, 2012). Östmark *et al.* (Ostmark et al., 2011) employed hyperspectral spontaneous Raman imaging for distinguishing explosives from inorganic particles, measuring circa 5 mm, at a distance of 10 m. The method was then successfully used to detect sulfur microparticles (20 μm) dispersed over a brick surface.

Bremer *et al.* (Bremer et al., 2011) used standoff CARS to identify explosives present in trace quantities in a complex chemical background – a polymer solution of PS and PMMA dispersed in toluene. The Raman images, recorded from a distance of 1 m, were not subject to any background subtraction or other processing procedures, yet regions rich in PMMA, PS and DNT (explosive) were clearly distinguishable, as shown in Figure 11.

[INSERT FIGURE 11 HERE]

Figure 11 – Stand-off Raman images created from a distance of 1 m showing trace detection in a complex environment. Title on each chemical image refers to the resonance monitored: PS = 1200 cm_1,

667 DNT=1350 cm_1, PMMA=1750 cm_1, and 2,6-DNT=1090 cm_1. Adapted from Applied Physics
668 Letters, 99:10, M.T. Bremer, P.J. Wrzesinski, N. Butcher et al., Highly selective standoff detection and
669 imaging of trace chemicals in a complex background using single-beam coherent anti-Stokes Raman,
670 101109, Copyright 2011, with the permission of AIP Publishing.

671 Standoff Raman techniques may be particularly interesting for monitoring MPs
672 in the ocean surface by passing ships or, indeed, for monitoring any surface with the aid
673 of a drone or a helicopter, as currently done in the search for explosives in enemy
674 territory using the LIDAR technology.

675

676

677 ## 7. Conclusions

678

679 This review outlined the major advantages and limitations of Raman
680 spectroscopy for the identification of environmental microplastics. Recently suggested
681 good practices for overcoming the well-known drawbacks of μ-Raman were discussed
682 and some possible future trends for MP analysis briefly introduced. In sum, μ-Raman
683 stands out as the method of choice for the non-destructive identification of very small
684 microplastics (<20 μm). Commonly cited drawbacks of Raman techniques, such as
685 weak signal and fluorescence interference, can be overcome by following appropriate
686 cleaning protocols, applying baseline removal algorithms and using more efficient
687 detectors. The development of automated Raman mapping routines enables fast
688 detection of plastic particles with minimal operator time. By streamlining particle pre-
689 selection, through particle detection software and, recently, fluorescent tagging of
690 microplastics, the number of data points to be collected is greatly

reduced without compromising representativeness. The current great challenge in microplastic identification is real-time monitoring, a goal achievable through the use of ultrafast, nonlinear Raman techniques such as stimulated Raman scattering which, when coupled with flow cytometry, proved feasible for high-throughput screening of plastic microbeads. The next decade promises to be a bustling period of activity for μ-Raman MP analysis. The authors of this review sincerely hope their humble contribution will further the completion of such project.

Acknowledgments

This work was developed within the scope of the project CICECO-Aveiro Institute of Materials, POCI-01-0145-FEDER-007679 (FCT Ref. UID /CTM /50011/2013), financed by portuguese funds through the FCT/MEC and when appropriate co-financed by FEDER under the PT2020 Partnership Agreement. FCT is gratefully acknowledged for funding a PhD grant to CFA (SFRH/BD/129040/2017) and a researcher contract under the program IF 2015 to MMN (IF/01468/2015).

References

Alexander, J., Barregard, L., Bignami, M., Ceccatelli, S., Cottrill, B., Dinovi, M., Edler, L., Grasl-Kraupp, B., Hogstrand, C., Hoogenboom, L., Knutsen, H.K., Nebbia, C.S., Oswald, I., Petersen, A., Rogiers, V.M., Rose, M., Roudot, A.-C., Schwerdtle, T., Vleminckx, C., Vollmer, G., Wallace, H., 2016. Presence of microplastics and nanoplastics in food, with particular focus on seafood. EFSA J. 14, 6, 4501, 1-30. https://doi.org/10.2903/j.efsa.2016.4501

Andor Technology, 2007. Optimizing an EMCCD for Spectroscopy [WWW Document]. Photonics Media. URL https://www.photonics.com/a31367 (accessed 5.21.18).

717 Andrady, A.L., 2017. The plastic in microplastics: A review. Mar. Pollut. Bull. 119, 12–22.
718 https://doi.org/10.1016/j.marpolbul.2017.01.082

719 Andrady, A.L., 2011. Microplastics in the marine environment. Mar. Pollut. Bull. 62, 1596–
720 1605. https://doi.org/10.1016/j.marpolbul.2011.05.030

721 Avio, C.G., Gorbi, S., Regoli, F., 2017. Plastics and microplastics in the oceans: From emerging
722 pollutants to emerged threat. Mar. Environ. Res. 128, 2–11.
723 https://doi.org/10.1016/j.marenvres.2016.05.012

724 Ballent, A., Corcoran, P.L., Madden, O., Helm, P.A., Longstaffe, F.J., 2016. Sources and sinks
725 of microplastics in Canadian Lake Ontario nearshore, tributary and beach sediments. Mar.
726 Pollut. Bull. 110, 383–395. https://doi.org/10.1016/j.marpolbul.2016.06.037

727 Beer, S., Garm, A., Huwer, B., Dierking, J., Nielsen, T.G., 2018. No increase in marine
728 microplastic concentration over the last three decades – A case study from the Baltic Sea. Sci.
729 Total Environ. 621, 1272–1279. https://doi.org/10.1016/j.scitotenv.2017.10.101

730 Blaesing, M., Amelung, W., 2018. Plastics in soil: Analytical methods and possible sources.
731 Sci. Total Environ. 612, 422–435. https://doi.org/10.1016/j.scitotenv.2017.08.086

732 Borman, S.A., 1982. Nonlinear Raman spectroscopy. Anal. Chem. 54, 1021A-1026A.
733 https://doi.org/10.1021/ac00246a002

734 Bremer, M.T., Wrzesinski, P.J., Butcher, N., Lozovoy, V.V., Dantus, M., 2011. Highly selective
735 standoff detection and imaging of trace chemicals in a complex background using single-beam
736 coherent anti-Stokes Raman scattering. Appl. Phys. Lett. 99, 101109.
737 https://doi.org/10.1063/1.3636436

738 Cai, L., Wang, J., Peng, J., Wu, Z., Tan, X., 2018. Observation of the degradation of three types
739 of plastic pellets exposed to UV irradiation in three different environments. Sci. Total Environ.
740 628–629, 740–747. https://doi.org/10.1016/j.scitotenv.2018.02.079

741 Clunies-Ross, P.J., Smith, G.P.S., Gordon, K.C., Gaw, S., 2016. Synthetic shorelines in New
742 Zealand? Quantification and characterisation of microplastic pollution on Canterbury's
743 coastlines. N. Z. J. Mar. Freshw. Res. 50, 317–325.
744 https://doi.org/10.1080/00288330.2015.1132747

745 Cole, M., Lindeque, P., Fileman, E., Halsband, C., Goodhead, R., Moger, J., Galloway, T.S.,
746 2013. Microplastic Ingestion by Zooplankton. Environ. Sci. Technol. 47, 6646–6655.
747 https://doi.org/10.1021/es400663f

748 Collard, F., Gilbert, B., Compere, P., Eppe, G., Das, K., Jauniaux, T., Parmentier, E., 2017a.
749 Microplastics in livers of European anchovies (Engraulis encrasicolus, L.). Environ. Pollut. 229,
750 1000–1005. https://doi.org/10.1016/j.envpol.2017.07.089

751 Collard, F., Gilbert, B., Eppe, G., Parmentier, E., Das, K., 2015. Detection of Anthropogenic
752 Particles in Fish Stomachs: An Isolation Method Adapted to Identification by Raman
753 Spectroscopy. Arch. Environ. Contam. Toxicol. 69, 331–339. https://doi.org/10.1007/s00244-
754 015-0221-0

755 Collard, F., Gilbert, B., Eppe, G., Roos, L., Compère, P., Das, K., Parmentier, E., 2017b.
756 Morphology of the filtration apparatus of three planktivorous fishes and relation with ingested
757 anthropogenic particles. Mar. Pollut. Bull. 116, 182–191.
758 https://doi.org/10.1016/j.marpolbul.2016.12.067

759 Conkle, J.L., Del Valle, C.D.B., Turner, J.W., 2018. Are We Underestimating Microplastic
760 Contamination in Aquatic Environments? Environ. Manage. 61, 1–8.
761 https://doi.org/10.1007/s00267-017-0947-8

762 Costa, J.P.D., Nunes, A.R., Santos, P.S.M., Girão, A.V., Duarte, A.C., Rocha-Santos, T., 2018.
763 Degradation of polyethylene microplastics in seawater: Insights into the environmental
764 degradation of polymers. J. Environ. Sci. Health Part A 0, 1–10.
765 https://doi.org/10.1080/10934529.2018.1455381

766 Cozar, A., Echevarria, F., Ignacio Gonzalez-Gordillo, J., Irigoien, X., Ubeda, B., Hernandez-
767 Leon, S., Palma, A.T., Navarro, S., Garcia-de-Lomas, J., Ruiz, A., Fernandez-de-Puelles, M.L.,
768 Duarte, C.M., 2014. Plastic debris in the open ocean. Proc. Natl. Acad. Sci. U. S. A. 111,
769 10239–10244. https://doi.org/10.1073/pnas.1314705111

770 Crawford, C.B., Quinn, B., 2017. 10 - Microplastic identification techniques, in: Microplastic
771 Pollutants. Elsevier, pp. 219–267. https://doi.org/10.1016/B978-0-12-809406-8.00010-4

772 da Costa, J.P., Santos, P.S.M., Duarte, A.C., Rocha-Santos, T., 2016. (Nano)plastics in the
773 environment - Sources, fates and effects. Sci. Total Environ. 566, 15–26.
774 https://doi.org/10.1016/j.scitotenv.2016.05.041

775 De Tender, C.A., Devriese, L.I., Haegeman, A., Maes, S., Ruttink, T., Dawyndt, P., 2015.
776 Bacterial Community Profiling of Plastic Litter in the Belgian Part of the North Sea. Environ.
777 Sci. Technol. 49, 9629–9638. https://doi.org/10.1021/acs.est.5b01093

778 Dehaut, A., Cassone, A.-L., Frere, L., Hermabessiere, L., Himber, C., Rinnert, E., Riviere, G.,
779 Lambert, C., Soudant, P., Huvet, A., Duflos, G., Paul-Pont, I., 2016. Microplastics in seafood:
780 Benchmark protocol for their extraction and characterization. Environ. Pollut. 215, 223–233.
781 https://doi.org/10.1016/j.envpol.2016.05.018

782 Di, M., Wang, J., 2018. Microplastics in surface waters and sediments of the Three Gorges
783 Reservoir, China. Sci. Total Environ. 616, 1620–1627.
784 https://doi.org/10.1016/j.scitotenv.2017.10.150

785 Dieing, T., Hollricher, O., 2008. High-resolution, high-speed confocal Raman imaging. Vib.
786 Spectrosc. 48, 22–27. https://doi.org/10.1016/j.vibspec.2008.03.004

787 Duis, K., Coors, A., 2016. Microplastics in the aquatic and terrestrial environment: sources
788 (with a specific focus on personal care products), fate and effects. Environ. Sci. Eur. 28:2.
789 https://doi.org/10.1186/s12302-015-0069-y

790 Elert, A.M., Becker, R., Duemichen, E., Eisentraut, P., Falkenhagen, J., Sturm, H., Braun, U.,
791 2017. Comparison of different methods for MP detection: What can we learn from them, and
792 why asking the right question before measurements matters? Environ. Pollut. 231, 1256–1264.
793 https://doi.org/10.1016/j.envpol.2017.08.074

794 Enders, K., Lenz, R., Beer, S., Stedmon, C.A., 2017. Extraction of microplastic from biota:
795 recommended acidic digestion destroys common plastic polymers. Ices J. Mar. Sci. 74, 326–
796 331. https://doi.org/10.1093/icesjms/fsw173

797 Enders, K., Lenz, R., Stedmon, C.A., Nielsen, T.G., 2015. Abundance, size and polymer
798 composition of marine microplastics >= 10 mu m in the Atlantic Ocean and their modelled
799 vertical distribution. Mar. Pollut. Bull. 100, 70–81.
800 https://doi.org/10.1016/j.marpolbul.2015.09.027

Eriksen, M., Lebreton, L.C.M., Carson, H.S., Thiel, M., Moore, C.J., Borerro, J.C., Galgani, F., Ryan, P.G., Reisser, J., 2014. Plastic Pollution in the World's Oceans: More than 5 Trillion Plastic Pieces Weighing over 250,000 Tons Afloat at Sea. PLOS ONE 9, e111913. https://doi.org/10.1371/journal.pone.0111913

Erni-Cassola, G., Gibson, M.I., Thompson, R.C., Christie-Oleza, J.A., 2017. Lost, but Found with Nile Red: A Novel Method for Detecting and Quantifying Small Microplastics (1 mm to 20 mu m) in Environmental Samples. Environ. Sci. Technol. 51, 13641–13648. https://doi.org/10.1021/acs.est.7b04512

Fischer, D., Kaeppler, A., Eichhorn, K.-J., 2015. Identification of Microplastics in the Marine Environment by Raman Microspectroscopy and Imaging. Am. Lab. 47, 32–34.

Frere, L., Paul-Pont, I., Moreau, J., Soudant, P., Lambert, C., Huvet, A., Rinnert, E., 2016. A semi-automated Raman micro-spectroscopy method for morphological and chemical characterizations of microplastic litter. Mar. Pollut. Bull. 113, 461–468. https://doi.org/10.1016/j.marpolbul.2016.10.051

Frere, L., Paul-Pont, I., Rinnert, E., Petton, S., Jaffre, J., Bihannic, I., Soudant, P., Lambert, C., Huvet, A., 2017. Influence of environmental and anthropogenic factors on the composition, concentration and spatial distribution of microplastics: A case study of the Bay of Brest (Brittany, France). Environ. Pollut. 225, 211–222. https://doi.org/10.1016/j.envpol.2017.03.023

Gago, J., Galgani, F., Maes, T., Thompson, R.C., 2016. Microplastics in Seawater: Recommendations from the Marine Strategy Framework Directive Implementation Process. Front. Mar. Sci. 3:219. https://doi.org/10.3389/fmars.2016.00219

Galloway, T.S., Dogra, Y., Garrett, N., Rowe, D., Tyler, C.R., Moger, J., Lammer, E., Landsiedel, R., Sauer, U.G., Scherer, G., Wohlleben, W., Wiench, K., 2017. Ecotoxicological assessment of nanoparticle-containing acrylic copolymer dispersions in fairy shrimp and zebrafish embryos. Environ. Sci.-Nano 4, 1981–1997. https://doi.org/10.1039/c7en00385d

Gares, K.L., Hufziger, K.T., Bykov, S.V., Asher, S.A., 2016. Review of explosive detection methodologies and the emergence of standoff deep UV resonance Raman. J. Raman Spectrosc. 47, 124–141. https://doi.org/10.1002/jrs.4868

Ghosal, S., Chen, M., Wagner, J., Wang, Z.-M., Wall, S., 2018. Molecular identification of polymers and anthropogenic particles extracted from oceanic water and fish stomach - A Raman micro-spectroscopy study. Environ. Pollut. 233, 1113–1124. https://doi.org/10.1016/j.envpol.2017.10.014

Goldstein, M.C., Goodwin, D.S., 2013. Gooseneck barnacles (Lepas spp.) ingest microplastic debris in the North Pacific Subtropical Gyre. Peerj 1, e184. https://doi.org/10.7717/peerj.184

Griffiths, P.R., Miseo, E.V., 2014. Infrared and Raman Instrumentation for Mapping and Imaging, in: Infrared and Raman Spectroscopic Imaging. Wiley-Blackwell, pp. 1–56. https://doi.org/10.1002/9783527678136.ch1

Gündoğdu, S., 2018. Contamination of table salts from Turkey with microplastics. Food Addit. Contam. Part A 0, 1–9. https://doi.org/10.1080/19440049.2018.1447694

Halstead, J.E., Smith, J.A., Carter, E.A., Lay, P.A., Johnston, E.L., 2018. Assessment tools for microplastics and natural fibres ingested by fish in an urbanised estuary. Environ. Pollut., 234, 552–561. https://doi.org/10.1016/j.envpol.2017.11.085

Hanvey, J.S., Lewis, P.J., Lavers, J.L., Crosbie, N.D., Pozo, K., Clarke, B.O., 2017. A review of analytical techniques for quantifying microplastics in sediments. Anal. Methods 9, 1369–1383. https://doi.org/10.1039/c6ay02707e

Hidalgo-Ruz, V., Gutow, L., Thompson, R.C., Thiel, M., 2012. Microplastics in the Marine Environment: A Review of the Methods Used for Identification and Quantification. Environ. Sci. Technol. 46, 3060–3075. https://doi.org/10.1021/es2031505

Horton, A.A., Jürgens, M.D., Lahive, E., Bodegom, P.M. van, Vijver, M.G., 2018. The influence of exposure and physiology on microplastic ingestion by the freshwater fish Rutilus rutilus (roach) in the River Thames, UK. Environ. Pollut. 236, 188–194. https://doi.org/10.1016/j.envpol.2018.01.044

Horton, A.A., Svendsen, C., Williams, R.J., Spurgeon, D.J., Lahive, E., 2017a. Large microplastic particles in sediments of tributaries of the River Thames, UK - Abundance, sources and methods for effective quantification. Mar. Pollut. Bull. 114, 218–226. https://doi.org/10.1016/j.marpolbul.2016.09.004

Horton, A.A., Walton, A., Spurgeon, D.J., Lahive, E., Svendsen, C., 2017b. Microplastics in freshwater and terrestrial environments: Evaluating the current understanding to identify the knowledge gaps and future research priorities. Sci. Total Environ. 586, 127–141. https://doi.org/10.1016/j.scitotenv.2017.01.190

Imhof, H.K., Ivleva, N.P., Schmid, J., Niessner, R., Laforsch, C., 2013. Contamination of beach sediments of a subalpine lake with microplastic particles. Curr. Biol. 23, R867–R868. https://doi.org/10.1016/j.cub.2013.09.001

Imhof, H.K., Laforsch, C., Wiesheu, A.C., Schmid, J., Anger, P.M., Niessner, R., Ivleva, N.P., 2016. Pigments and plastic in limnetic ecosystems: A qualitative and quantitative study on microparticles of different size classes. Water Res. 98, 64–74. https://doi.org/10.1016/j.watres.2016.03.015

Imhof, H.K., Schmid, J., Niessner, R., Ivleva, N.P., Laforsch, C., 2012. A novel, highly efficient method for the separation and quantification of plastic particles in sediments of aquatic environments. Limnol. Oceanogr.-Methods 10, 524–537. https://doi.org/10.4319/lom.2012.10.524

Imhof, H.K., Wiesheu, A.C., Anger, P.M., Niessner, R., Ivleva, N.P., Laforsch, C., 2018. Variation in plastic abundance at different lake beach zones - A case study. Sci. Total Environ. 613, 530–537. https://doi.org/10.1016/j.scitotenv.2017.08.300

Ivleva, N.P., Wiesheu, A.C., Niessner, R., 2017. Microplastic in Aquatic Ecosystems. Angew. Chem.-Int. Ed. 56, 1720–1739. https://doi.org/10.1002/anie.201606957

Jahnke, A., Arp, H.P.H., Escher, B.I., Gewert, B., Gorokhova, E., Kühnel, D., Ogonowski, M., Potthoff, A., Rummel, C., Schmitt-Jansen, M., Toorman, E., MacLeod, M., 2017. Reducing Uncertainty and Confronting Ignorance about the Possible Impacts of Weathering Plastic in the Marine Environment. Environ. Sci. Technol. Lett. 4, 85–90. https://doi.org/10.1021/acs.estlett.7b00008

Jiang, J.-Q., 2018. Occurrence of microplastics and its pollution in the environment: A review. Sustain. Prod. Consum. 13, 16–23. https://doi.org/10.1016/j.spc.2017.11.003

Kaeppler, A., Fischer, D., Oberbeckmann, S., Schernewski, G., Labrenz, M., Eichhorn, K.-J., Voit, B., 2016. Analysis of environmental microplastics by vibrational microspectroscopy:

FTIR, Raman or both? Anal. Bioanal. Chem. 408, 8377–8391. https://doi.org/10.1007/s00216-016-9956-3

Kaeppler, A., Windrich, F., Loeder, M.G.J., Malanin, M., Fischer, D., Labrenz, M., Eichhorn, K.-J., Voit, B., 2015. Identification of microplastics by FTIR and Raman microscopy: a novel silicon filter substrate opens the important spectral range below 1300 cm(-1) for FTIR transmission measurements. Anal. Bioanal. Chem. 407, 6791–6801. https://doi.org/10.1007/s00216-015-8850-8

Karami, A., Golieskardi, A., Choo, C.K., Larat, V., Galloway, T.S., Salamatinia, B., 2017a. The presence of microplastics in commercial salts from different countries. Sci. Rep. 7:46173. https://doi.org/10.1038/srep46173

Karami, A., Golieskardi, A., Choo, C.K., Larat, V., Karbalaei, S., Salamatinia, B., 2018. Microplastic and mesoplastic contamination in canned sardines and sprats. Sci. Total Environ. 612, 1380–1386. https://doi.org/10.1016/j.scitotenv.2017.09.005

Karami, A., Golieskardi, A., Choo, C.K., Romano, N., Bin Ho, Y., Salamatinia, B., 2017b. A high-performance protocol for extraction of microplastics in fish. Sci. Total Environ. 578, 485–494. https://doi.org/10.1016/j.scitotenv.2016.10.213

Karami, A., Golieskardi, A., Ho, Y.B., Larat, V., Salamatinia, B., 2017c. Microplastics in eviscerated flesh and excised organs of dried fish. Sci. Rep. 7:5473. https://doi.org/10.1038/s41598-017-05828-6

Karami, A., Romano, N., Galloway, T., Hamzah, H., 2016. Virgin microplastics cause toxicity and modulate the impacts of phenanthrene on biomarker responses in African catfish (Clarias gariepinus). Environ. Res. 151, 58–70. https://doi.org/10.1016/j.envres.2016.07.024

Karlsson, T.M., Vethaak, A.D., Almroth, B.C., Ariese, F., van Velzen, M., Hassellov, M., Leslie, H.A., 2017. Screening for microplastics in sediment, water, marine invertebrates and fish: Method development and microplastic accumulation. Mar. Pollut. Bull. 122, 403–408. https://doi.org/10.1016/j.marpolbul.2017.06.081

Klein, S., Dimzon, I.K., Eubeler, J., Knepper, T.P., 2018. Analysis, Occurrence, and Degradation of Microplastics in the Aqueous Environment, in: Wagner, M., Lambert, S. (Eds.), Freshwater Microplastics : Emerging Environmental Contaminants? Springer International Publishing, Cham, pp. 51–67. https://doi.org/10.1007/978-3-319-61615-5_3

Lares, M., Ncibi, M.C., Sillanpää, Markus, Sillanpää, Mika, 2018. Occurrence, identification and removal of microplastic particles and fibers in conventional activated sludge process and advanced MBR technology. Water Res. 133, 236–246. https://doi.org/10.1016/j.watres.2018.01.049

Lawson, L.S., Rodriguez, J.D., 2016. Raman Barcode for Counterfeit Drug Product Detection. Anal. Chem. 88, 4706–4713. https://doi.org/10.1021/acs.analchem.5b04636

Lei, K., Qiao, F., Liu, Q., Wei, Z., Qi, H., Cui, S., Yue, X., Deng, Y., An, L., 2017. Microplastics releasing from personal care and cosmetic products in China. Mar. Pollut. Bull. 123, 122–126. https://doi.org/10.1016/j.marpolbul.2017.09.016

Lenz, R., Enders, K., Stedmon, C.A., Mackenzie, D.M.A., Nielsen, T.G., 2015. A critical assessment of visual identification of marine microplastic using Raman spectroscopy for analysis improvement. Mar. Pollut. Bull. 100, 82–91. https://doi.org/10.1016/j.marpolbul.2015.09.026

Li, J., Liu, H., Chen, J.P., 2017. Microplastics in freshwater systems: A review on occurrence, environmental effects, and methods for microplastics detection. Water Res. 137, 362-374 https://doi.org/10.1016/j.watres.2017.12.056

Liao, C.-S., Wang, P., Huang, C.Y., Lin, P., Eakins, G., Bentley, R.T., Liang, R., Cheng, J.-X., 2017. In Vivo and in Situ Spectroscopic Imaging by a Handheld Stimulated Raman Scattering Microscope. ACS Photonics 5, 947–954. https://doi.org/10.1021/acsphotonics.7b01214

Liboiron, F., Ammendolia, J., Saturno, J., Melvin, J., Zahara, A., Richárd, N., Liboiron, M., 2018. A zero percent plastic ingestion rate by silver hake (Merluccius bilinearis) from the south coast of Newfoundland, Canada. Mar. Pollut. Bull. 131, 267–275. https://doi.org/10.1016/j.marpolbul.2018.04.007

Loeder, M.G.J., Gerdts, G., 2015. Methodology Used for the Detection and Identification of Microplastics—A Critical Appraisal, in: Bergmann, M., Gutow, L., Klages, M. (Eds.), Marine Anthropogenic Litter. Springer International Publishing, Cham, pp. 201–227. https://doi.org/10.1007/978-3-319-16510-3_8

Loeder, M.G.J., Kuczera, M., Mintenig, S., Lorenz, C., Gerdts, G., 2015. Focal plane array detector-based micro-Fourier-transform infrared imaging for the analysis of microplastics in environmental samples. Environ. Chem. 12, 563–581. https://doi.org/10.1071/EN14205

Lots, F.A.E., Behrens, P., Vijver, M.G., Horton, A.A., Bosker, T., 2017. A large-scale investigation of microplastic contamination: Abundance and characteristics of microplastics in European beach sediment. Mar. Pollut. Bull. 123, 219–226. https://doi.org/10.1016/j.marpolbul.2017.08.057

Lusher, A.L., Burke, A., O'Connor, I., Officer, R., 2014. Microplastic pollution in the Northeast Atlantic Ocean: Validated and opportunistic sampling. Mar. Pollut. Bull. 88, 325–333. https://doi.org/10.1016/j.marpolbul.2014.08.023

Lusher, A.L., Welden, N.A., Sobral, P., Cole, M., 2017. Sampling, isolating and identifying microplastics ingested by fish and invertebrates. Anal. Methods 9, 1346–1360. https://doi.org/10.1039/c6ay02415g

Maes, T., Jessop, R., Wellner, N., Haupt, K., Mayes, A.G., 2017. A rapid-screening approach to detect and quantify microplastics based on fluorescent tagging with Nile Red. Sci. Rep. 7: 44501. https://doi.org/10.1038/srep44501

Mai, L., Bao, L.-J., Shi, L., Wong, C.S., Zeng, E.Y., 2018. A review of methods for measuring microplastics in aquatic environments. Environ. Sci. Pollut. Res. 25, 11319–11332. https://doi.org/10.1007/s11356-018-1692-0

Miller, M.E., Kroon, F.J., Motti, C.A., 2017. Recovering microplastics from marine samples: A review of current practices. Mar. Pollut. Bull. 123, 6–18. https://doi.org/10.1016/j.marpolbul.2017.08.058

Mintenig, S.M., Int-Veen, I., Loeder, M.G.J., Primpke, S., Gerdts, G., 2017. Identification of microplastic in effluents of waste water treatment plants using focal plane array-based micro-Fourier-transform infrared imaging. Water Res. 108, 365–372. https://doi.org/10.1016/j.watres.2016.11.015

Muhlschlegel, P., Hauk, A., Walter, U., Sieber, R., 2017. Lack of evidence for microplastic contamination in honey. Food Addit. Contam. Part -A 34, 1982–1989. https://doi.org/10.1080/19440049.2017.1347281

Murray, F., Cowie, P.R., 2011. Plastic contamination in the decapod crustacean Nephrops norvegicus (Linnaeus, 1758). Mar. Pollut. Bull. 62, 1207–1217. https://doi.org/10.1016/j.marpolbul.2011.03.032

Naidu, S.A., Ranga Rao, V., Ramu, K., 2018. Microplastics in the benthic invertebrates from the coastal waters of Kochi, Southeastern Arabian Sea. Environ. Geochem. Health. https://doi.org/10.1007/s10653-017-0062-z

Oberbeckmann, S., 2017. BONUS MICROPOLL - Multilevel assessment of microplastics and associated pollutants in the Baltic Sea [WWW Document]. URL https://www.io-warnemuende.de/micropoll-home.html (accessed 5.17.18).

Ogonowski, M., Gerdes, Z., Gorokhova, E., 2018. What we know and what we think we know about microplastic effects – A critical perspective. Curr. Opin. Environ. Sci. Health 1, 41–46. https://doi.org/10.1016/j.coesh.2017.09.001

Opilik, L., Schmid, T., Zenobi, R., 2013. Modern Raman Imaging: Vibrational Spectroscopy on the Micrometer and Nanometer Scales. Annu. Rev. Anal. Chem. 6, 379–398. https://doi.org/10.1146/annurev-anchem-062012-092646

Ossmann, B.E., Sarau, G., Schmitt, S.W., Holtmannspoetter, H., Christiansen, S.H., Dicke, W., 2017. Development of an optimal filter substrate for the identification of small microplastic particles in food by micro-Raman spectroscopy. Anal. Bioanal. Chem. 409, 4099–4109. https://doi.org/10.1007/s00216-017-0358-y

Ostmark, H., Nordberg, M., Carlsson, T.E., 2011. Stand-off detection of explosives particles by multispectral imaging Raman spectroscopy. Appl. Opt. 50, 5592–5599. https://doi.org/10.1364/AO.50.005592

Palmer, A., Phapale, P., Fay, D., Alexandrov, T., 2017. Curatr: a web application for creating, curating and sharing a mass spectral library. Bioinformatics 34, 1436-1438. https://doi.org/10.1093/bioinformatics/btx786

Qiu, Q., Tan, Z., Wang, J., Peng, J., Li, M., Zhan, Z., 2016. Extraction, enumeration and identification methods for monitoring microplastics in the environment. Estuar. Coast. Shelf Sci. 176, 102–109. https://doi.org/10.1016/j.ecss.2016.04.012

Remy, F., Collard, F., Gilbert, B., Compere, P., Eppe, G., Lepoint, G., 2015. When Microplastic Is Not Plastic: The Ingestion of Artificial Cellulose Fibers by Macrofauna Living in Seagrass Macrophytodetritus. Environ. Sci. Technol. 49, 11158–11166. https://doi.org/10.1021/acs.est.5b02005

Renner, G., Schmidt, T.C., Schram, J., 2018. Analytical methodologies for monitoring micro(nano)plastics: Which are fit for purpose? Curr. Op. Env. Sci. Hea1th 1, 55–61. https://doi.org/10.1016/j.coesh.2017.11.001

Revel, M., Châtel, A., Mouneyrac, C., 2018. Micro(nano)plastics: A threat to human health? Curr. Op. Env. Sci. Hea1th 1, 17–23. https://doi.org/10.1016/j.coesh.2017.10.003

Ribeiro-Claro, P., Nolasco, M.M., Araújo, C., 2017. Chapter 5 - Characterization of Microplastics by Raman Spectroscopy, in: Rocha-Santos, T.A.P., Duarte, A.C. (Eds.), Comprehensive Analytical Chemistry, Characterization and Analysis of Microplastics. Elsevier, pp. 119–151. https://doi.org/10.1016/bs.coac.2016.10.001

1013 Rocha-Santos, T., Duarte, A.C., 2015. A critical overview of the analytical approaches to the
1014 occurrence, the fate and the behavior of microplastics in the environment. Trac-Trends Anal.
1015 Chem. 65, 47–53. https://doi.org/10.1016/j.trac.2014.10.011

1016 Rodrigues, M.O., Abrantes, N., Gonçalves, F.J.M., Nogueira, H., Marques, J.C., Gonçalves,
1017 A.M.M., 2018. Spatial and temporal distribution of microplastics in water and sediments of a
1018 freshwater system (Antuã River, Portugal). Sci. Total Environ. 633, 1549–1559.
1019 https://doi.org/10.1016/j.scitotenv.2018.03.233

1020 Rodríguez-Seijo, A., Pereira, R., 2017. Chapter 3 - Morphological and Physical
1021 Characterization of Microplastics, in: Rocha-Santos, T.A.P., Duarte, A.C. (Eds.),
1022 Characterization and Analysis of Microplastics, Comprehensive Analytical Chemistry. Elsevier,
1023 pp. 49–66. https://doi.org/10.1016/bs.coac.2016.10.007

1024 Scheurer, M., Bigalke, M., 2018. Microplastics in Swiss Floodplain Soils. Environ. Sci.
1025 Technol. 52, 3591–3598. https://doi.org/10.1021/acs.est.7b06003

1026 Schmaelzlin, E., Moralejo, B., Rutowska, M., Monreal-Ibero, A., Sandin, C., Tarcea, N., Popp,
1027 J., Roth, M.M., 2014. Raman Imaging with a Fiber-Coupled Multichannel Spectrograph.
1028 Sensors 14, 21968–21980. https://doi.org/10.3390/s141121968

1029 Schymanski, D., Goldbeck, C., Humpf, H.-U., Fürst, P., 2018. Analysis of microplastics in
1030 water by micro-Raman spectroscopy: Release of plastic particles from different packaging into
1031 mineral water. Water Res. 129, 154–162. https://doi.org/10.1016/j.watres.2017.11.011

1032 Shan, J., Zhao, J., Liu, L., Zhang, Y., Wang, X., Wu, F., 2018. A novel way to rapidly monitor
1033 microplastics in soil by hyperspectral imaging technology and chemometrics. Environ. Pollut.
1034 238, 121–129. https://doi.org/10.1016/j.envpol.2018.03.026

1035 Shim, W.J., Hong, S.H., Eo, S.E., 2017. Identification methods in microplastic analysis: a
1036 review. Anal. Methods 9, 1384–1391. https://doi.org/10.1039/c6ay02558g

1037 Shim, W.J., Song, Y.K., Hong, S.H., Jang, M., 2016. Identification and quantification of
1038 microplastics using Nile Red staining. Mar. Pollut. Bull. 113, 469–476.
1039 https://doi.org/10.1016/j.marpolbul.2016.10.049

1040 Silva, A.B., Bastos, A.S., Justino, C.I.L., da Costa, J.P., Duarte, A.C., Rocha-Santos, T.A.P.,
1041 2018. Microplastics in the environment: Challenges in analytical chemistry - A review. Anal.
1042 Chim. Acta 1017, 1-19. https://doi.org/10.1016/j.aca.2018.02.043

1043 Smith, W.E., Dent, G., 2005. Modern Raman Spectroscopy: A Practical Approach. John Wiley
1044 & Sons, Ltd, West Sussex, England.

1045 Song, Y.K., Hong, S.H., Jang, M., Han, G.M., Rani, M., Lee, J., Shim, W.J., 2015. A
1046 comparison of microscopic and spectroscopic identification methods for analysis of
1047 microplastics in environmental samples. Mar. Pollut. Bull. 93, 202–209.
1048 https://doi.org/10.1016/j.marpolbul.2015.01.015

1049 Sruthy, S., Ramasamy, E.V., 2017. Microplastic pollution in Vembanad Lake, Kerala, India:
1050 The first report of microplastics in lake and estuarine sediments in India. Environ. Pollut. 222,
1051 315–322. https://doi.org/10.1016/j.envpol.2016.12.038

1052 Stewart, S., Priore, R.J., Nelson, M.P., Treado, P.J., 2012. Raman Imaging. Annu. Rev. Anal.
1053 Chem. 5, 337–360. https://doi.org/10.1146/annurev-anchem-062011-143152

1054 Sujathan, S., Kniggendorf, A.-K., Kumar, A., Roth, B., Rosenwinkel, K.-H., Nogueira, R.,
1055 2017. Heat and Bleach: A Cost-Efficient Method for Extracting Microplastics from Return

Activated Sludge. Arch. Environ. Contam. Toxicol. 73, 641–648. https://doi.org/10.1007/s00244-017-0415-8

Syakti, A.D., 2017. Microplastics Monitoring in Marine Environment. Omni-Akuatika 13, 1-6. https://doi.org/10.20884/1.oa.2017.13.2.430

Tagg, A.S., Sapp, M., Harrison, J.P., Ojeda, J.J., 2015. Identification and Quantification of Microplastics in Wastewater Using Focal Plane Array-Based Reflectance Micro-FT-IR Imaging. Anal. Chem. 87, 6032–6040. https://doi.org/10.1021/acs.analchem.5b00495

Van Cauwenberghe, L., Claessens, M., Vandegehuchte, M.B., Janssen, C.R., 2015. Microplastics are taken up by mussels (Mytilus edulis) and lugworms (Arenicola marina) living in natural habitats. Environ. Pollut. 199, 10–17. https://doi.org/10.1016/j.envpol.2015.01.008

Van Cauwenberghe, L., Janssen, C.R., 2014. Microplastics in bivalves cultured for human consumption. Environ. Pollut. 193, 65–70. https://doi.org/10.1016/j.envpol.2014.06.010

Van Cauwenberghe, L., Vanreusel, A., Mees, J., Janssen, C.R., 2013. Microplastic pollution in deep-sea sediments. Environ. Pollut. 182, 495–499. https://doi.org/10.1016/j.envpol.2013.08.013

Wagner, J., Wang, Z.-M., Ghosal, S., Rochman, C., Gassel, M., Wall, S., 2017. Novel method for the extraction and identification of microplastics in ocean trawl and fish gut matrices. Anal. Methods 9, 1479–1490. https://doi.org/10.1039/c6ay02396g

Watts, A.J.R., Lewis, C., Goodhead, R.M., Beckett, S.J., Moger, J., Tyler, C.R., Galloway, T.S., 2014. Uptake and Retention of Microplastics by the Shore Crab Carcinus maenas. Environ. Sci. Technol. 48, 8823–8830. https://doi.org/10.1021/es501090e

Watts, A.J.R., Urbina, M.A., Goodhead, R., Moger, J., Lewis, C., Galloway, T.S., 2016. Effect of Microplastic on the Gills of the Shore Crab Carcinus maenas. Environ. Sci. Technol. 50, 5364–5369. https://doi.org/10.1021/acs.est.6b01187

Wiesheu, A.C., Anger, P.M., Baumann, T., Niessner, R., Ivleva, N.P., 2016. Raman microspectroscopic analysis of fibers in beverages. Anal. Methods 8, 5722–5725. https://doi.org/10.1039/c6ay01184e

Wright, S.L., Kelly, F.J., 2017. Plastic and Human Health: A Micro Issue? Environ. Sci. Technol. 51, 6634–6647. https://doi.org/10.1021/acs.est.7b00423

Wu, C., Zhang, K., Xiong, X., 2018. Microplastic Pollution in Inland Waters Focusing on Asia, in: Wagner, M., Lambert, S. (Eds.), Freshwater Microplastics : Emerging Environmental Contaminants? Springer International Publishing, Cham, pp. 85–99. https://doi.org/10.1007/978-3-319-61615-5_5

Xiong, X., Zhang, K., Chen, X., Shi, H., Luo, Z., Wu, C., 2018. Sources and distribution of microplastics in China's largest inland lake – Qinghai Lake. Environ. Pollut. 235, 899–906. https://doi.org/10.1016/j.envpol.2017.12.081

Yonkos, L.T., Friedel, E.A., Perez-Reyes, A.C., Ghosal, S., Arthur, C.D., 2014. Microplastics in Four Estuarine Rivers in the Chesapeake Bay, USA. Environ. Sci. Technol. 48, 14195–14202. https://doi.org/10.1021/es5036317

Young, A.M., Elliott, J.A., 2016. Characterization of microplastic and mesoplastic debris in sediments from Kamilo Beach and Kahuku Beach, Hawai'i. Mar. Pollut. Bull. 113, 477–482. https://doi.org/10.1016/j.marpolbul.2016.11.009

1098 Yu, Y., Zhou, D., Li, Z., Zhu, C., 2018. Advancement and Challenges of Microplastic Pollution
1099 in the Aquatic Environment: a Review. Water. Air. Soil Pollut. 229, 140.
1100 https://doi.org/10.1007/s11270-018-3788-z

1101 Zada, L., Leslie, H.A., Vethaak, A.D., Tinnevelt, G., Janssen, J., Boer, J.F. de, Ariese, F., 2018.
1102 Fast microplastics identification with stimulated Raman scattering microscopy. J. Raman
1103 Spectrosc. Special Issue, 1-9 https://doi.org/10.1002/jrs.5367

1104 Zettler, E.R., Mincer, T.J., Amaral-Zettler, L.A., 2013. Life in the "Plastisphere": Microbial
1105 Communities on Plastic Marine Debris. Environ. Sci. Technol. 47, 7137–7146.
1106 https://doi.org/10.1021/es401288x

1107 Zhang, C., Huang, K.-C., Rajwa, B., Li, J., Yang, S., Lin, H., Liao, C., Eakins, G., Kuang, S.,
1108 Patsekin, V., Robinson, J.P., Cheng, J.-X., 2017. Stimulated Raman scattering flow cytometry
1109 for label-free single-particle analysis. Optica 4, 103–109.
1110 https://doi.org/10.1364/OPTICA.4.000103

1111 Zhang, K., Su, J., Xiong, X., Wu, X., Wu, C., Liu, J., 2016. Microplastic pollution of lakeshore
1112 sediments from remote lakes in Tibet plateau, China. Environ. Pollut. 219, 450–455.
1113 https://doi.org/10.1016/j.envpol.2016.05.048

1114 Zhang, K., Xiong, X., Hu, H., Wu, C., Bi, Y., Wu, Y., Zhou, B., Lam, P.K.S., Liu, J., 2017.
1115 Occurrence and Characteristics of Microplastic Pollution in Xiangxi Bay of Three Gorges
1116 Reservoir, China. Environ. Sci. Technol. 51, 3794–3801.
1117 https://doi.org/10.1021/acs.est.7b00369

1118 Zhao, S., Danley, M., Ward, J.E., Li, D., Mincer, T.J., 2017. An approach for extraction,
1119 characterization and quantitation of microplastic in natural marine snow using Raman
1120 microscopy. Anal. Methods 9, 1470–1478. https://doi.org/10.1039/c6ay02302a

1121 Zhao, S., Zhu, L., Li, D., 2015. Microplastic in three urban estuaries, China. Environ. Pollut.
1122 206, 597–604. https://doi.org/10.1016/j.envpol.2015.08.027

1123

Highlights

Raman is the method of choice for identifying small microplastics (<20 μm)

Automated mapping routines and library matching allow fast microplastic detection

Nonlinear Raman techniques enable real-time monitoring of microplastics

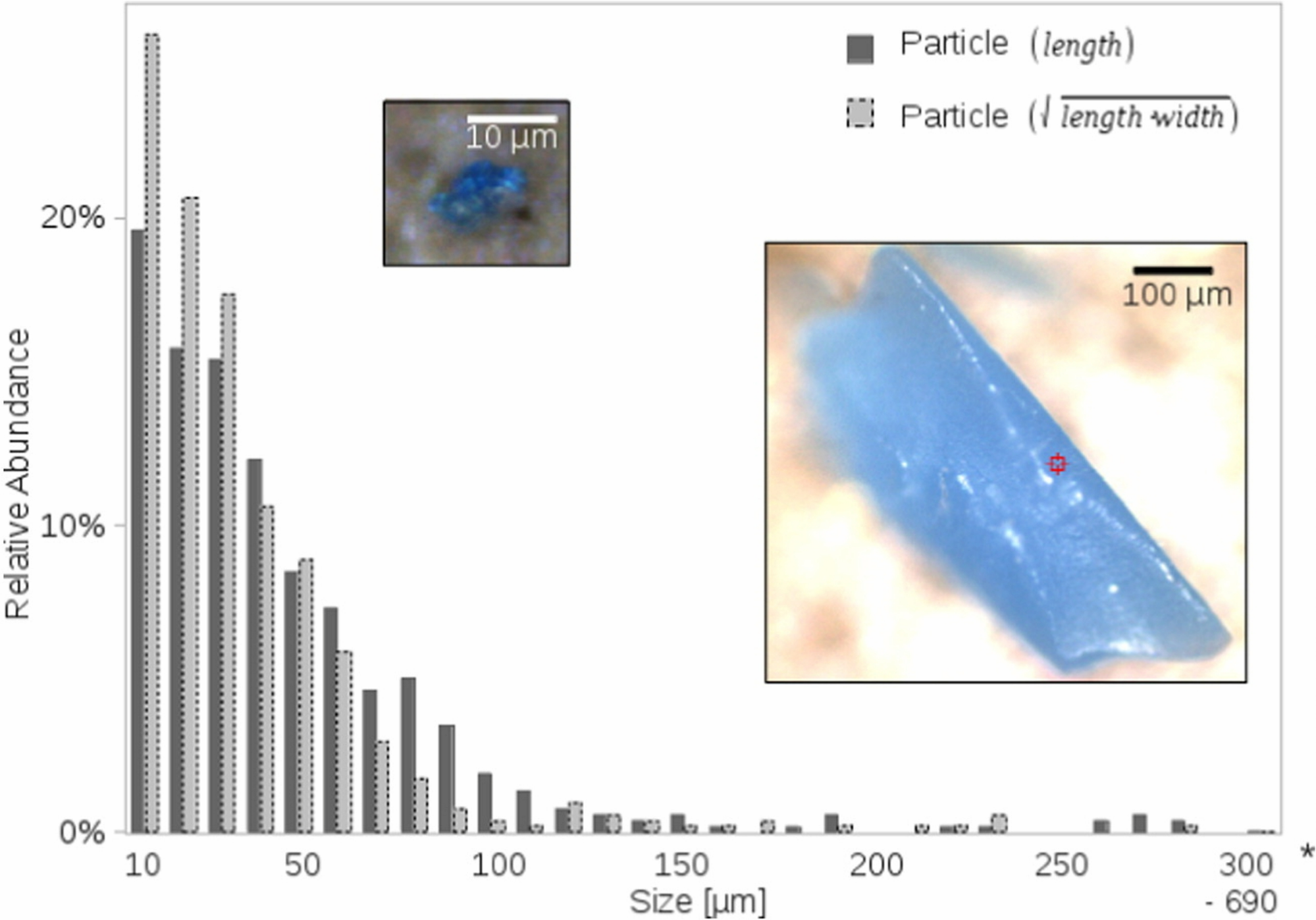
Particle (length)
Particle ($\sqrt{length \cdot width}$)
10 µm
100 µm
20%
10%
0%
Relative Abundance
10
50
100
150
200
250
300
*
Size [µm]
- 690

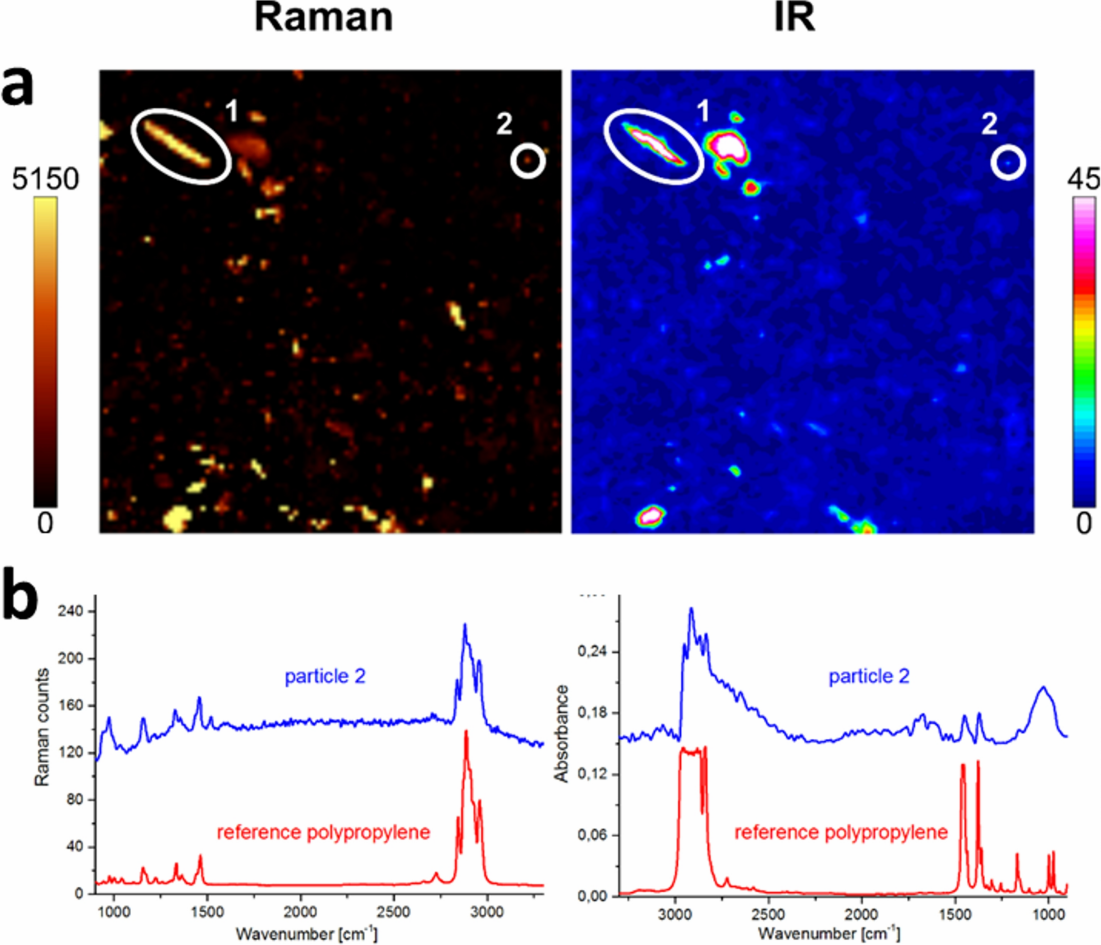
Raman
IR
a
1
2
5150
0
45
0
b
particle 2
reference polypropylene
Raman counts
Wavenumber [cm-1]
Absorbance
Wavenumber [cm-1]

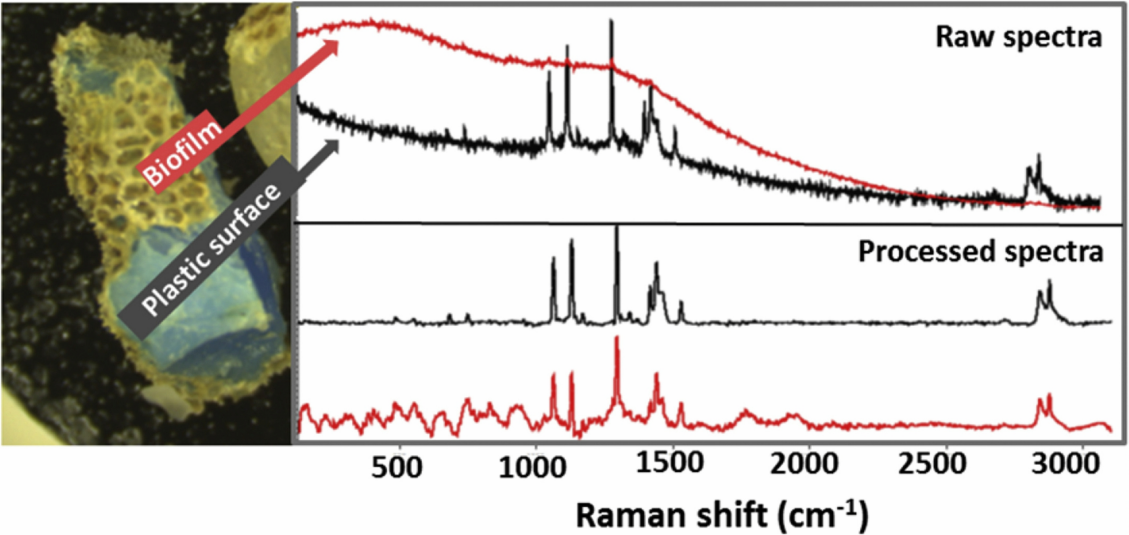
Biofilm
Plastic surface
Raw spectra
Processed spectra
500
1000
1500
2000
2500
3000
Raman shift (cm-1)

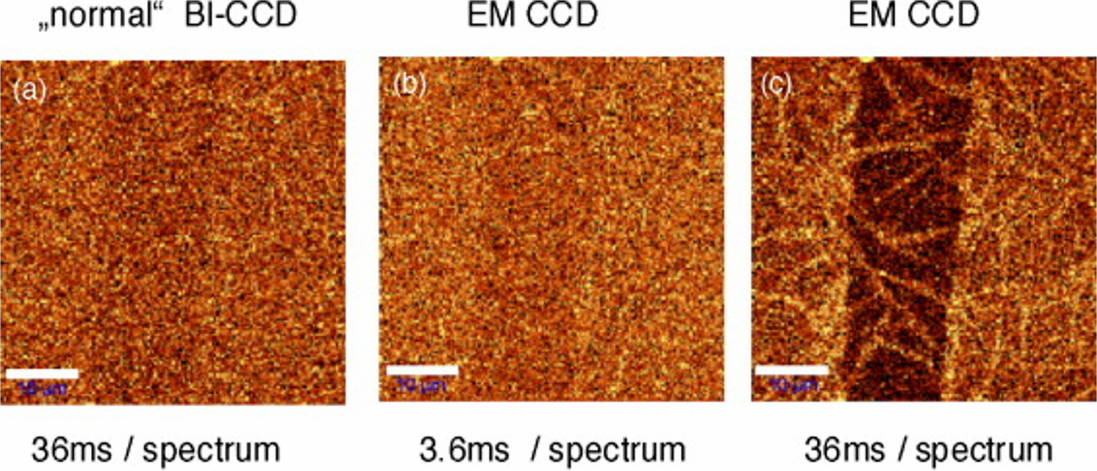
„normal“ BI-CCD
EM CCD
EM CCD
(a)
(b)
(c)
36ms / spectrum
3.6ms / spectrum
36ms / spectrum
(d)
PMMA
contamination
glass
7.1 nm PMMA + 4.2 nm contamination on glass

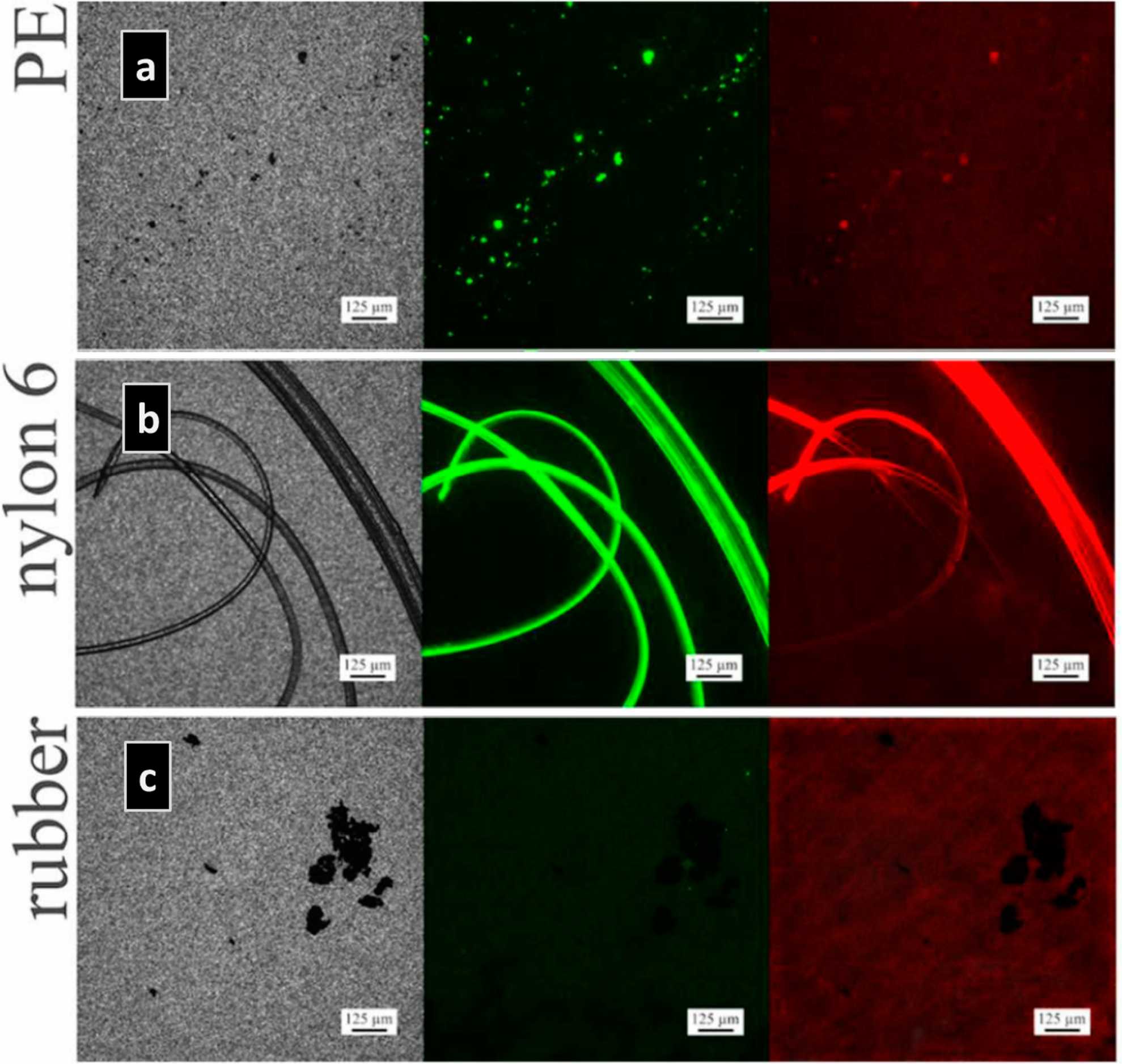
PE
a
125 µm
125 µm
125 µm
nylon 6
b
125 µm
125 µm
125 µm
rubber
c
125 µm
125 µm
125 µm

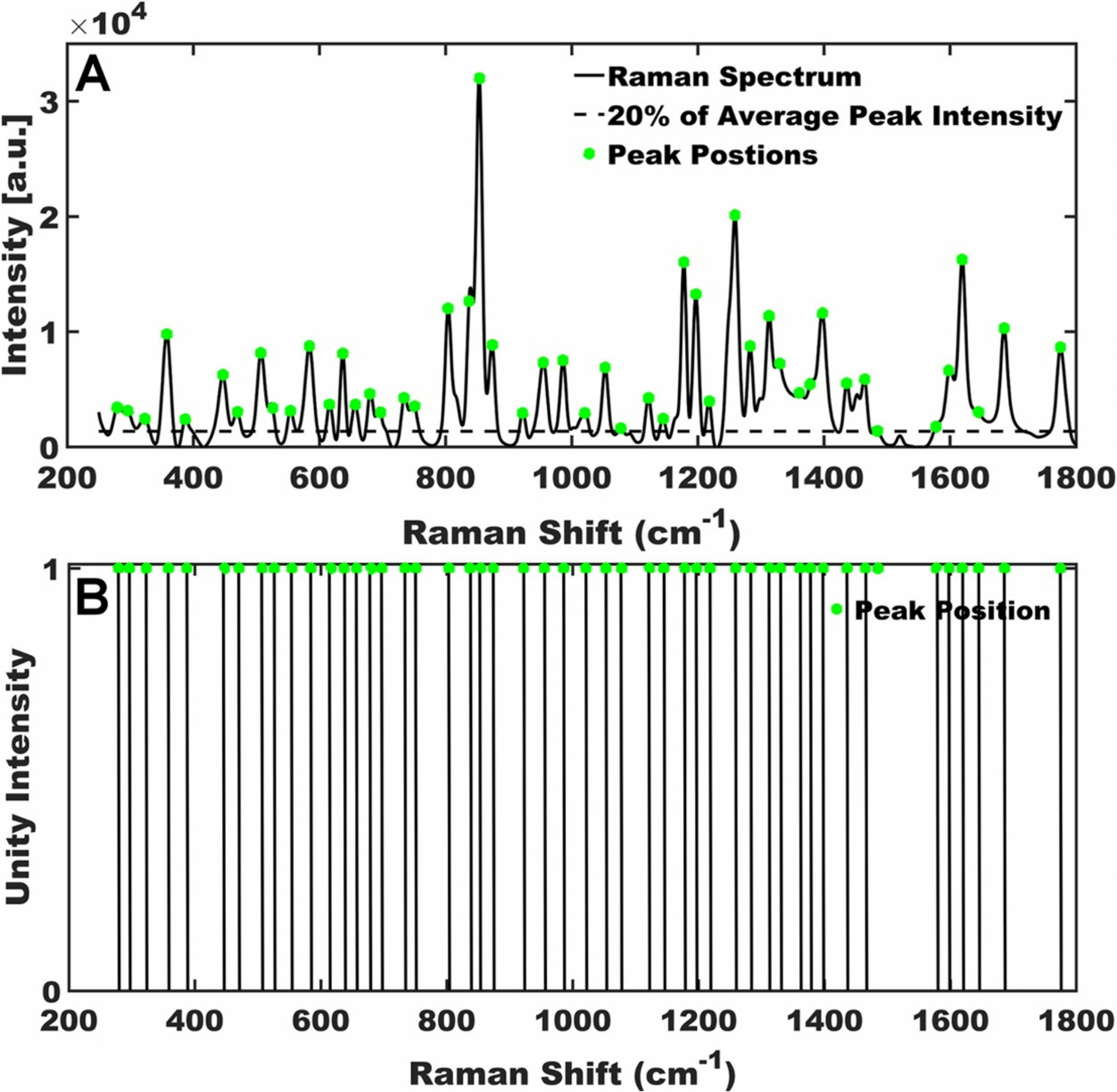
A
×10^4
Raman Spectrum
20% of Average Peak Intensity
Peak Postions
Intensity [a.u.]
0
1
2
3
200
400
600
800
1000
1200
1400
1600
1800
Raman Shift (cm^-1)
B
Peak Position
Unity Intensity
0
1
200
400
600
800
1000
1200
1400
1600
1800
Raman Shift (cm^-1)

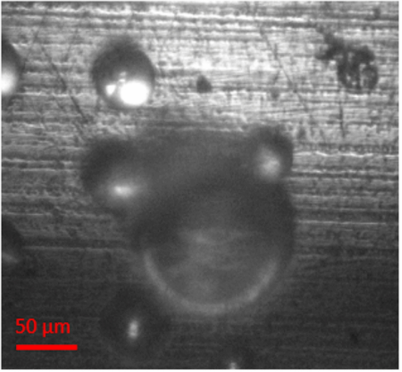
50 µm

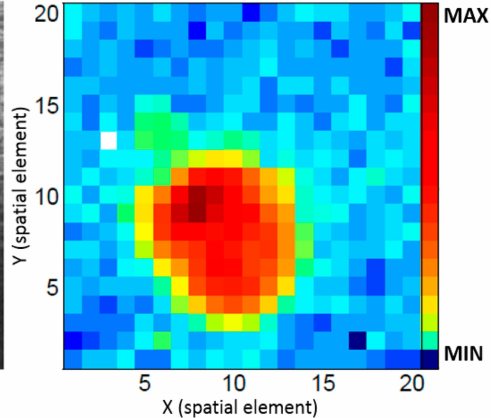
20
15
10
5
Y (spatial element)
5
10
15
20
X (spatial element)
MAX
MIN

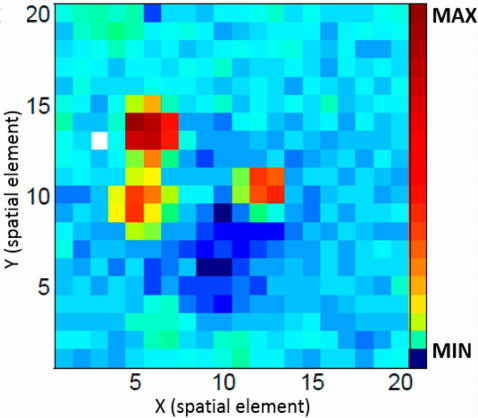
20
15
10
5
Y (spatial element)
5
10
15
20
X (spatial element)
MAX
MIN

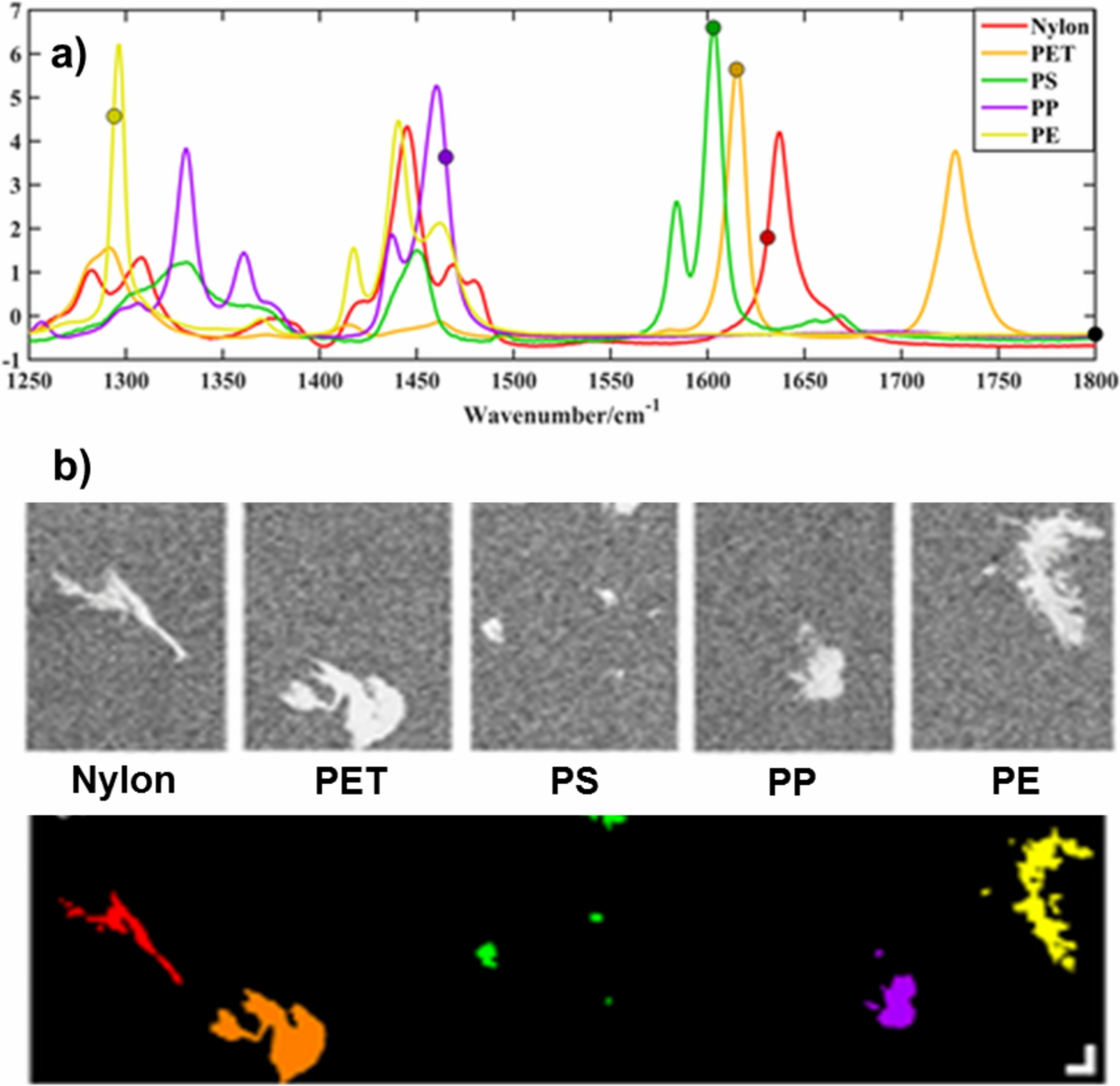
a)
Nylon
PET
PS
PP
PE
7
6
5
4
3
2
1
0
-1
1250
1300
1350
1400
1450
1500
1550
1600
1650
1700
1750
1800
Wavenumber/cm-1
b)
Nylon
PET
PS
PP
PE

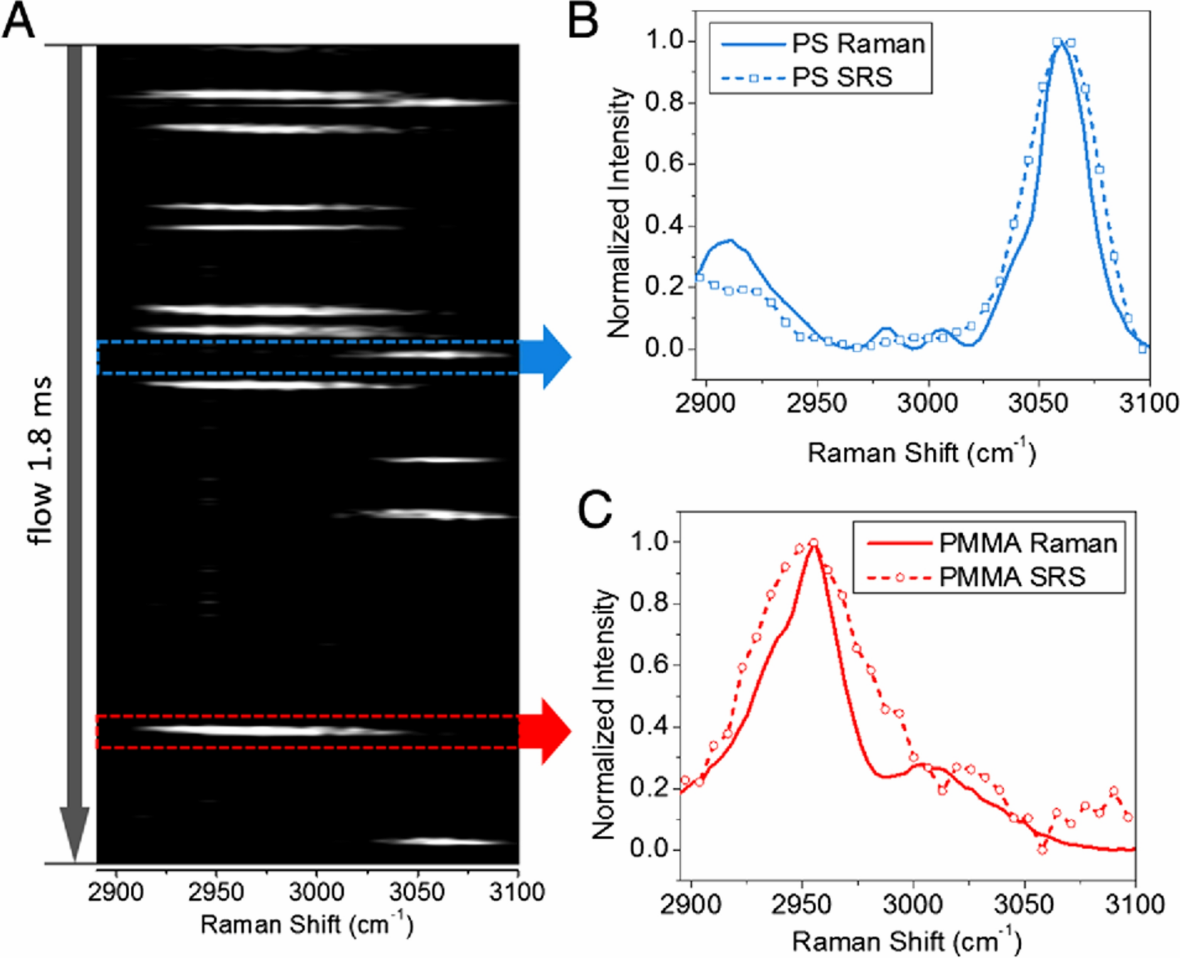
A
flow 1.8 ms
2900
2950
3000
3050
3100
Raman Shift (cm-1)
B
PS Raman
PS SRS
Normalized Intensity
1.0
0.8
0.6
0.4
0.2
0.0
2900
2950
3000
3050
3100
Raman Shift (cm-1)
C
PMMA Raman
PMMA SRS
Normalized Intensity
1.0
0.8
0.6
0.4
0.2
0.0
2900
2950
3000
3050
3100
Raman Shift (cm-1)

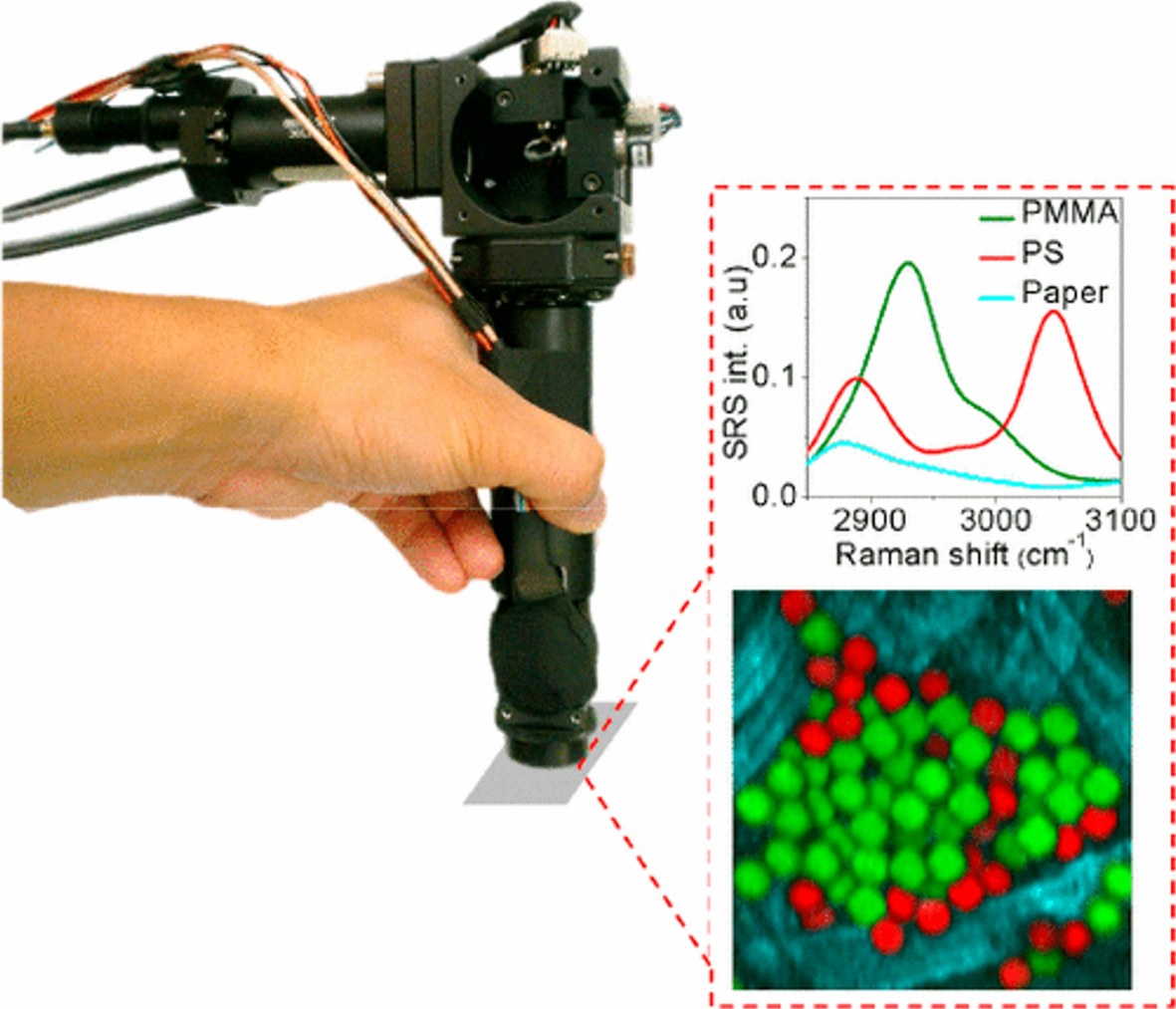
PMMA
PS
Paper
SRS int. (a.u)
0.0
0.1
0.2
2900
3000
3100
Raman shift (cm-1)

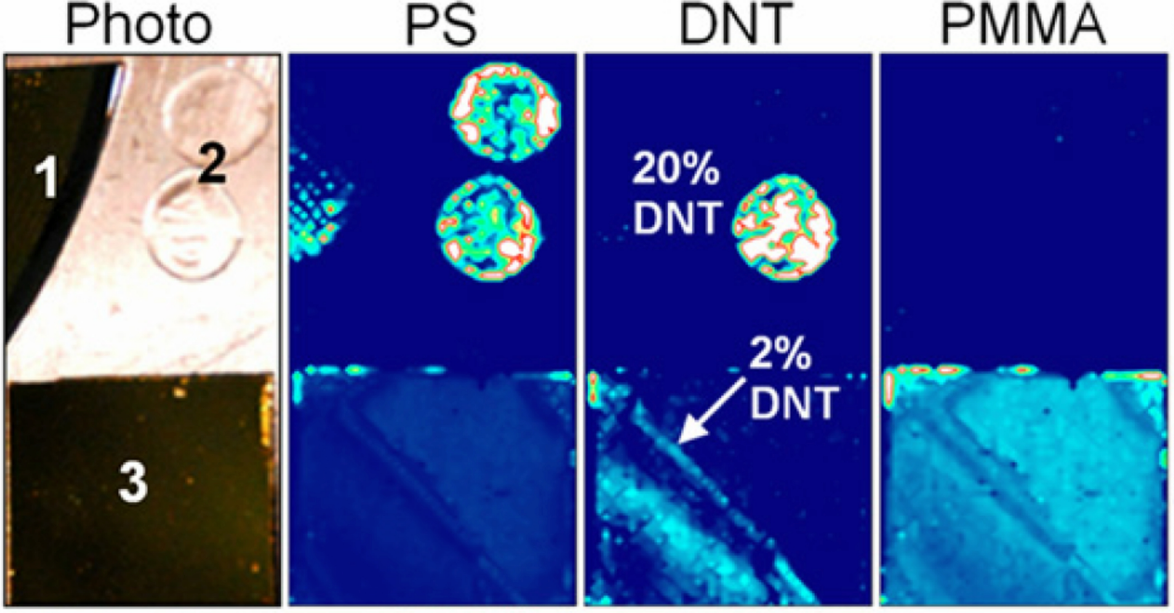
Photo
PS
DNT
PMMA
1
2
3
20%
DNT
2%
DNT

*MICROPLASTICS + **RAMAN** = IDENTIFICATION*

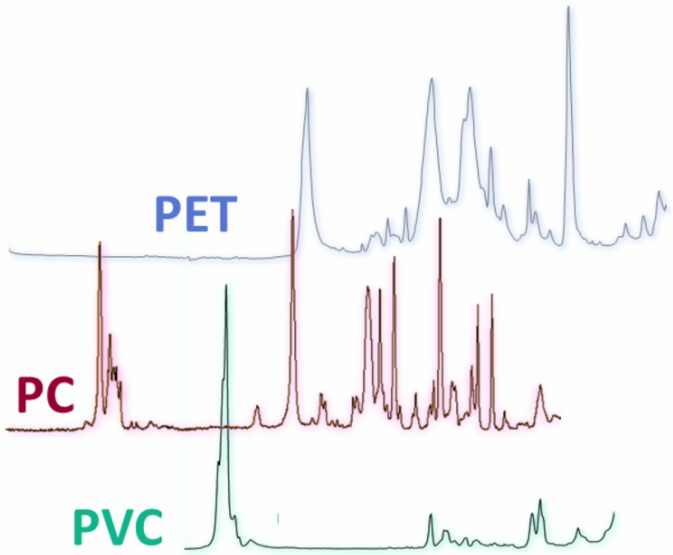

BETTER ✓

FASTER ✓

STRONGER ✓